UCRL-17433

University of California

Ernest O. Lawrence Radiation Laboratory

HIGH-ENERGY-PHYSICS EXPERIMENTS WITH POLARIZED TARGETS

Berkeley, California

Paper presented at the Saclay (France) Conference
on Polarized Targets and Ion Sources,
December 1966.

UCRL-17433
Preprint

UNIVERSITY OF CALIFORNIA

Lawrence Radiation Laboratory
Berkeley, California

AEC Contract No. W-7405-eng-48

HIGH-ENERGY-PHYSICS EXPERIMENTS WITH POLARIZED TARGETS

Owen Chamberlain

December 1966

HIGH-ENERGY-PHYSICS EXPERIMENTS WITH POLARIZED TARGETS

Owen Chamberlain

December 1966

If we are to do a workmanlike job of studying the strong interactions it is imperative that we have knowledge of the spin dependence of the forces. This implies that polarization experiments are essential. Already Bareyre, Bricman, Stirling and Villet[1] have shown that pion-proton polarization experiments should be interpreted as indicating two new resonances not previously seen by other methods.

The present-day approach to determining detailed pion-proton scattering amplitudes is to use measured differential cross sections, polarization measurements, dispersion relations, and isospin conservation rules. Further assumptions are unitarity of the S matrix and the short-range nature of strong interactions. In the more distant future I hope we may see the day when the scattering experiments will be sufficiently detailed that the dispersion relations will not be necessary to the interpretation of results. Then the dispersion relations may themselves be checked experimentally, rather than being assumed.

I see, then, an early period of polarization experiments followed by a later period in which more extensive experimental results will be called for. For the pion-proton system the first period seems well progressed, based on measurements of differential cross section and P , the polarization. In the second period more complex experiments should be required, such as measurements of the parameters R and A . In R and A measurements, the protons have a known polarization before the collision takes place. After the pion scatters on the proton, one asks how much residual polarization the proton has.

The nucleon-nucleon (N-N) system is susceptible to similar analysis, but there are more amplitudes to be determined, so more experiments must be performed. The N-N system is less well analyzed at present than the π-N system.

Before describing in detail the experiments that have already been performed we review the definition of polarization, restricting our discussion to particles of spin 1/2. If a beam or target has random spin-axis directions it is said to be unpolarized. If all the spin axes are oriented in a particular direction it is said to be completely (or 100%) polarized in that direction. For any beam or target we may imagine that we measure the component of spin along a particular direction for each particle, finding for each particle either $+\frac{1}{2}$ (spin up along the chosen direction) or $-\frac{1}{2}$ (spin down). The component of polarization in the chosen direction is then

$$P = \frac{N_{up} - N_{down}}{N_{up} + N_{down}}$$

where N_{up} (or N_{down}) is the number with spin up (or down).

The first experiment performed with a polarized proton target was that of Abragam, Borghini, Catillon, Coustham, Roubeau, and Thirion.[2] It was a measurement of the parameter C_{nn} for proton-proton scattering at 20 MeV. The parameter C_{nn} is a spin correlation coefficient expressing the dependence of the differential scattering cross section on the relative spin orientation of two colliding protons. The subscripts n refer to the normal to the scattering plane. We imagine first that a proton beam completely polarized in a particular direction normal to its direction of motion impinges on a proton target completely polarized either parallel or antiparallel to the polarization direction of the beam. In either case let $I(\theta)$ be the differential cross section for scattering in a plane perpendicular (normal) to the polarization direction at center-of-mass angle θ. The parameter C_{nn} would then be

$$C_{nn}(\theta) = \frac{I_{\text{parallel}}(\theta) - I_{\text{antiparallel}}(\theta)}{I_{\text{parallel}}(\theta) + I_{\text{antiparallel}}(\theta)} .$$

If the beam polarization is P_B and the target polarization P_T then the equivalent expression is

$$C_{nn}(\theta) = \frac{1}{P_B} \frac{1}{P_T} \frac{I_{\text{parallel}}(\theta) - I_{\text{antiparallel}}(\theta)}{I_{\text{parallel}}(\theta) + I_{\text{antiparallel}}(\theta)} .$$

A sketch of the experimental arrangement of Abragam et al. is shown in Fig. 1. A beam of α particles was incident at the left on a hydrogenous foil, giving rise to knock-on protons highly polarized in a vertical direction (normal to the scattering plane at the hydrogenous foil, the first target). The highly polarized protons (of 20 MeV) impinged on a polarized proton target (of lanthanum magnesium nitrate (LMN)) and proton-proton scattering events were counted at center-of-mass angles between 60° and 90°. By measuring the rate of p-p scattering events with the target protons polarized parallel or antiparallel to the beam polarization, they could determine C_{nn}. For the proton-proton system the meaning of C_{nn} is particularly simple at 90° c.m. scattering angle: Spins parallel means triplet spin state; spins antiparallel means singlet. The experimental value of -0.91 for C_{nn} corresponds to the fact that the p-p scattering at this energy is mainly in singlet states. However, as the scattering angle deviates from 90°(c.m.) the interpretation becomes more complicated.

Since I attribute to Professors Abragam and Jeffries the birth of polarized proton targets in usable form, it would be fitting if I next described work of which Professor Jeffries is a co-author. However, I want first to give the definition of the relevant parameter P and then to describe the older technique of measuring it.

The definition of the polarization parameter P is the final-state polarization after the scattering process providing the particles were unpolarized before the scattering. In fact Fig. 2 shows a plan view of an experiment[3] to measure the parameter P by rescattering the recoil protons from a π-p collision. A pion beam strikes the (unpolarized) hydrogen target. The recoil protons are rescattered on a second (carbon) target, where any vertical component of polarization would result in a left-right asymmetry in the scattering at the carbon target. This is a tolerable way to measure P if no more convenient way is readily available. While some improvements on this basic method have been made with the introduction of spark chambers,[4] it is still better to use a different approach that involves a polarized proton target.

The use of a polarized target to measure P depends on the presumed facts that the strong interactions conserve parity and are invariant under the time-reversal transformation. We will not make the arguments here, but they may be found in a review paper of Wolfenstein.[5] The result is that for elastic scattering the left-right asymmetry ϵ of the scattering on a target completely polarized up is numerically equal to P :

$$\epsilon \equiv \frac{N_{left}-N_{right}}{N_{left}+N_{right}} = P$$

where N_{left} (or N_{right}) is the number of pions elastically scattered to the left (or right) at angle θ and P is the polarization in scattering at the same angle. If the target is not 100% polarized this may be corrected for by using

$$\epsilon = P_T P$$

where P_T is the target polarization. By measuring P_T and the asymmetry ϵ we may deduce P .

In practice one of the two configurations (let us say that of right scattering) can be rotated by 180° around the beam direction so that the counter is on the left but the target polarized down. This has the advantage that the counter may be in exactly the same position for the two cases being compared, so there is no problem of making a left scattering angle exactly equal to a right scattering angle. The desired asymmetry is then

$$\epsilon = \frac{N_{up}-N_{down}}{N_{up}+N_{down}}$$

where N_{up} (or N_{down}) is the number of scattering processes detected in a counter to the left when the target is polarized up (or down). This is the method used by Jeffries, Schultz, Shapiro, Van Rossum and myself.[6]

A further comment is necessary concerning the separation of pion-proton scattering events from other types of scattering such as pion scattering by protons bound in complex nuclei. When the target material is lanthanum magnesium double nitrate (LMN) the protons of hydrogen constitute only 3 percent of the target weight. Accordingly, scattering by bound protons is much more common than scattering by free protons (hydrogen). To avoid having the interesting events overshadowed by unwanted scattering processes one must select elastic pion-proton scatterings from other scattering processes on the basis of the scattering kinematics.

The selection of elastic scattering processes on free hydrogen can be accomplished by steps as follows:

a) Observe whether a scattered pion is accompanied by a coplanar recoil proton, as required by the elastic scattering on hydrogen,

b) Observe whether the angle of emission of the coplanar recoil proton is that expected for elastic scattering kinematics,

c) Check whether the energy of the emerging pion is consistent with kinematics, and

d) See whether the energy of the recoil proton is consistent with the kinematics.

If all of these checks were applied, the background would be small indeed, as witnessed by the very-high-momentum-transfer p-p scattering experiments at alternating-gradient synchrotrons.[7] In practice it is often sufficient to apply (a) and (b) only, and is much simpler. That is the way most of the π-p scattering experiments were done.

Figure 3 shows the apparatus. A coincidence between the pion telescope and some proton counter indicated a coplanar event (condition (a)), and a coincidence with the central proton counter indicated the proton angle was consistent with π-p scattering. Scattering by bound protons is rather like scattering from a moving nucleon, so the emergence angle of the proton is usually not that of elastic scattering on free hydrogen.

Figure 4 shows a further elaboration of the same method in which the scattered beam particle may be detected in any one of 10 counters above the beam line, and the recoil proton detected in one of 10 counters below. Figure 5 shows a typical histogram constructed out of the scattered particles from a polarized target made of LMN. Each event that registered in a particular upper counter (number 6) has been entered in the histogram if it was coincident with a count in one of the ten lower counters so as to show the number of coincidence counts in each of the lower counters. The figure shows 3 sets of data: counts taken with the target negatively polarized (opposite to the termal equilibrium direction), counts taken with target positively polarized, and counts taken with a dummy target, chosen to be similar to LMN except having no hydrogen content. The polarized target data show a strong peak due to free hydrogen above a broad background from heavy elements in the LMN. The dummy-target data allow a reasonable subtraction of the background to be made. Notice that the size of the hydrogen peak is slightly different for the two signs of target polarization, indicating some asymmetry in the scattering process in this case.

Figure 6 shows the results of Betz et al.[8] on the polarization in proton-proton scattering at 740 MeV, as an illustration of typical results. Figure 7 shows their results at 328 MeV, compared to earlier results at 310 MeV obtained without benefit of polarized target. The agreement is not perfect but, within the recognizable errors, indicates that we may have confidence in the measurement of the target polarization in this case.

Figure 8 shows results of Grannis et al.[9] for polarization in p-p scattering at higher energy.

Figure 9 displays the largest value of polarization in p-p scattering as a function of the (laboratory) kinetic energy. After it reaches a peak value near 700 MeV it decreases monotonically at higher energy, in qualitative agreement with theoretical expectations.

When it is desired to use the polarized target for a measurement of polarization at a very small angle it may be impracticable to make the target thin enough that the recoil proton can emerge reliably. In this case one is restricted to making measurements only on the scattered beam particle to distinguish the scattering from free hydrogen. A case in point is taken from reference 6, where polarization in small-angle pion-proton scattering was attempted. The method consists in measuring the energy of pions scattered at a particular angle and selecting those whose energy is consistent with elastic scattering kinematics. In this case the range of the pions in a copper absorber could be used as a measure of their energy. Figure 10 shows differential range curves taken with LMN target and with dummy target. The difference shows the elastic scattering on hydrogen, but notice that for data taken at the appropriate value of copper absorber the LMN counts are only about 20% due to hydrogen, the rest being background from heavy elements. This indicates the limitations on the use of a polarized LMN target when only one constraint can be applied to distinguish the scattering on free hydrogen.

An arrangement for measuring C_{nn} in proton-proton scattering is shown in Fig. 11. It is the apparatus of Dost et al.[10] The 740-MeV external beam from the cyclotron is deflected by two magnets so as to impinge on the first target of liquid hydrogen either from above or from below the regular beam line. The protons that go in the forward direction are polarized in the scattering and may be focussed onto the polarized hydrogen target (of LMN). In order to determine C_{nn} without altering the counter positions one takes a 4-way difference involving both signs of beam polarization, by striking the liquid hydrogen target both from above and from below, and both signs of polarization in the LMN target. The expression is

$$C_{nn} = \frac{1}{P_T} \frac{1}{P_B} \frac{N_{++}-N_{+-}-N_{-+}+N_{--}}{N_{++}+N_{+-}+N_{-+}+N_{--}}$$

where T indicates target (LMN), B indicates beam (incident on the LMN target) and the other subscripts refer to incident-beam polarization direction and polarized-target polarization direction. The results are shown in Fig. 12, along with three points obtained by Golovin, Dzhelepov, Zul'karneev, and Wa-Ch'uang[11] without the benefit of a polarized target. The agreement between the two experiments is quite good. The fact that C_{nn} is nearly 1 at 90° indicates that the scattering there is mostly triplet scattering.

A very important series of measurements on pion-proton polarization has been made by Atkinson, Cox, Duke, Heard, Jones, Kemp, Murphy, Prentice, and Thresher.[12] Their apparatus is shown in Fig. 13. It uses an extensive series of counters on each side of the beam. Figure 14 shows a view of their apparatus viewed along the beam direction. They have used an extensive array of counters to assure the coplanarity of the events they have used in their results. They have made measurements at a number of energies. Figure 15 shows typical results, for the case of incident pion momentum of 1080 MeV/c. These results have played a crucial part in the analysis of Bareyre, Bricman, Stirling, and Villet,[1]

Similar experiments have been carried out at a somewhat higher energy of π-p scattering by Suwa, Yokosawa, Booth, Esterling, and Hill.[14] Their experimental arrangement is shown in Fig. 16, and Fig. 17 shows their "hydrogen peak", in the histogram of coincidence counts between the counters of one array with a particular counter in the other array. An example of their results is shown in Fig. 18.

A recently used arrangement of Hansroul et al.[15] is shown in elevation view in Fig. 19. Some 30 counters above the beam partly overlap each adjacent counter so as to give some 60 "bins" of angle in the scattering plane. Counters below the beam line are similarly arranged. Not shown in the figure are like sets of counters running in a perpendicular direction so that when a particle strikes the plane of a counter array both its coordinates can be recorded. This system should combine good coplanarity determination and good angular resolution with a large solid angle for counting scattered particles. Some trouble was experienced with electrons in the pion beam. It was found that electrons may emit high-energy X rays in the first part of the LMN target and these X rays may then make electron-positron pairs in the latter part of the target. The pairs go almost directly forward, but the magnetic field of the polarized-target magnet deflects one member of the pair up into one counter array and the other down into the other counter array. Because these electron-pair events tend to satisfy the coplanarity requirement automatically, they can represent a troublesome background. It was also found that it is helpful to have the polarized target rather completely surrounded with anticoincidence counters in directions in which the desired events do not send particles. At high energy the anticoincidence counters help to suppress unwanted inelastic processes. Measurements were made at 10 energies for the π^--p polarization and 15 energies for the π^+-p . As an example of some of the better results, Fig. 20 shows the results for incident momentum 1.44 GeV/c.

We have said above that for elastic scattering the asymmetry observed in scattering on a polarized target is guaranteed by parity conservation and time-reversal invariance to be related to the polarization P in the same scattering process by

$$\epsilon = P_T P \quad .$$

Bilen'kii[16] has pointed out that if the character of the particles changes in the scattering process we may have the more general relation

$$\epsilon = \pm P_T P$$

where the plus sign applies if there is no change in the intrinsic parity of the particles involved in the scattering, the minus sign if the intrinsic parity changes.

As an example, consider the reaction

$$\pi + p \rightarrow K^+ + \Sigma^+ \quad .$$

Both the pion and the K meson have zero spin and both proton and Σ hyperon have spin 1/2, so this is a suitable place to apply the Bilen'kii argument. If the product of π and p intrinsic parities is the same (or different) from the product of K and Σ intrinsic parities we will have a plus (or minus) sign in the relation

$$\epsilon = \pm P_T P \quad .$$

P has already been measured in bubble-chamber experiments so a measurement of asymmetry ϵ in the reaction on a polarized target could check the product of intrinsic parities of K and Σ. (The π-p system is already known to have an odd product of intrinsic parities.)

In spite of the fact that the K-Σ parity was believed demonstrated to be odd, on the basis of work by Tripp et al.[17] Dieterle et al.[18] in Berkeley decided to remeasure the K-Σ parity as a demonstration of the new method and as a further reassurance about the Tripp result. The apparatus used is shown in Fig. 21. The incident pion beam was partially separated to suppress protons. Pion momenta were measured in spark chambers and magnets along the beam line. The desired reaction was selected by the observation of a final-state K^+ particle, detected in a somewhat standard K^+detector involving K^+ that come to rest in a water Cherenkov counter. By observing the K^+ angle of emission (by spark chambers) and the K^+ energy (by range measurement) the authors could obtain a one-constraint selection of the desired reaction. Figure 22 shows more detail of the apparatus in the vicinity of the water Cherenkov counter. Two prior Cherenkov counters were required to show no pulse (the desired K mesons being too slow to produce Cherenkov light there) but the large water Cherenkov was required to show a delayed pulse (due to the fast decay products of the K^+). The range of the K^+ was determined by extrapolating forward the spark-chamber track of the entering K^+ particle and extrapolating backward the decay product as observed in the "μ" spark chamber.

For each stopping K^+ a parameter was calculated to compare the observed energy with that expected from kinematic relations for the desired reaction for a K^+ emitted at the angle observed for that event. To construct this parameter each stopping K^+ was treated as if it originated from free hydrogen but as if the unobserved particle were not necessarily a Σ particle, but some fictitious particle of mass m (missing mass). When this missing mass falls close to the mass of a Σ^+ the event is consistent with the desired reaction.

Figure 23 shows the distribution in missing mass for the observed events from the polarized target (of LMN). There is certainly no clear hydrogen peak in the vicinity of the Σ mass. Rather, there is a broad distribution more characteristic of the heavy elements in the target. When the LMN target was replaced with a CH_2 target the resulting missing mass distribution did show a hydrogen peak, as shown in Fig. 24. This indicated that the apparatus was performing as expected and allowed one to make a computation of the fraction of free-hydrogen events in the polarized-target data. On the basis of this analysis these data confirm the odd parity of the K-Σ system rather than even parity by odds of 40 to 1. The experiment indicated again the difficulties of working with one-constraint fits to separate the hydrogen effect in the LMN target.

A conceptually similar experiment designed to measure the intrinsic parity of the Ξ hyperon is in the analysis stage at the CERN laboratory.

A valuable extension in the uses of a polarized proton target has been made by a Saclay-Orsay-Pisa collaboration, as reported by Sonderegger at the Stony Brook Conference. They have used a polarized target to measure the polarization in charge-exchange scattering

$$\pi^- + p \rightarrow \pi^0 + n$$

particularly at high energy and small momentum transfer to the nucleon. Figure 25 shows their experimental arrangement. They observe the neutron and measure its velocity by time of flight in scintillation counters and they observe the gamma rays from the decay of the neutral pion in spark chambers. Their trigger is based on an incident negative pion, no charged particle emerging from the target, and the detection of a reasonably slow neutron. Their separation of a hydrogen peak is quite clear in Fig. 26. Their results are shown in Fig. 27, for incident pion momenta of 5.9 and 11.2 GeV/c. This process is quite interesting in that the polarization had been expected to vanish rapidly at high energy according to the simplest Regge-pole model.

Extensive high-energy polarization measurements have been made for π-p and p-p scattering by a group of CERN authors consisting of Borghini, Coignet, Dick, Kuroda, di Lella, Macq, Michalowicz and Olivier. They used incident momenta from 6 to 12 GeV/c. Because of the high incident energy the measurements are limited to the most forward directions of scattering. However, there is a great deal of interest in this near-forward scattering as it contains vital information on the limiting behavior of scattering amplitudes at high energy. In particular, it is important to decide whether Regge poles are sufficient to describe the high-energy scattering at small angles. Other more complex polarization experiments will also be needed but the measurement of P is a very important first step. One form of their experimental arrangement is shown in Fig. 28. They have used a counter hodoscope to determine the angle of scattering of the beam particle and have used an ingenious substitute, which I will not discuss here, to determine the angle of the recoil proton. Their hydrogen peaks are shown in part in Fig. 29. Their results for π-p polarization are shown in Fig. 30. In all cases the data for π^+-p polarization are positive at small angles, those for π^--p are negative at small angles. The curves are the theoretical values of Chiu, Phillips, and Rarita[19] based upon a Regge-pole analysis. The agreement with the Regge analysis is not bad. The experimental results for p-p scattering are shown as solid circles in Fig. 31. At 6 GeV/c there is not perfect agreement with results obtained in Berkeley.

I have omitted descriptions of some other quite interesting applications of polarized proton targets such as their use to obtain relatively high-intensity polarized neutron beams, as reported by Dragicescu, Lushchikov, Nikolenko, Taran, and Shapiro.[20] Incidentally, this work suggests that for targets of high polarization it may be practicable to measure the target polarization by measuring the transmission of the target to an initially unpolarized beam of slow neutrons.

Several other valuable polarized-target experiments are now under way. K-p polarization experiments are now well started at CERN and at the Rutherford Laboratory, and work is well progressed at Saclay toward measurements of the parameters A and R for π-p scattering. While many of the experiments previously mentioned could have been done, if necessary, without polarized proton targets, the measurements of A and R definitely require polarized targets. Here is an important aspect of scattering for which polarized targets are absolutely essential.

It is my expectation that we will hear during this conference about promising possibilities for target materials other than the presently predominant LMN. There is a particular need for polarized targets with a higher proportion of hydrogen, and for some experiments it will be important to have targets less susceptible to radiation damage than LMN. I look forward to hearing the current status of new target materials and I hope this conference will lead to further work toward finding superior new target materials.

REFERENCES

1. Bareyre, Bricman, Stirling, and Villet, Phys. Lett. 18, 342 (1965).
2. Abragam, Borghini, Catillon, Coustham, Roubeau, and Thirion, Phys. Lett. 2, 310 (1962).
3. Foote, Chamberlain, Rogers, Steiner, Wiegand, and Ypsilantis, Phys. Rev. 122, 948 (1961); Foote, Chamberlain, Rogers, and Steiner, Phys. Rev. 122, 959 (1961); Rogers, Chamberlain, Foote, Steiner, Wiegand, and Ypsilantis, Rev. Mod. Phys. 33, 356 (1961).
4. See, for example, Bareyre, Bricman, Longo, Valladas, Villet, Bizard, Duchon, Fontaine, Patry, Seguinot, and Yonnet, Phys. Rev. Lett. 14, 198 (1965), or Eandi, Devlin, Kenney, McManigal, and Moyer, Phys. Rev. 136, B536 (1964).
5. Lincoln Wolfenstein, Ann. Rev. Nuclear Sci. 6, 43 (1956).
6. Chamberlain, Jeffries, Schultz, Shapiro, and Van Rossum, Phys. Lett. 7, 293 (1963).
7. See, for example, Cocconi, Cocconi, Krisch, Orear, Rubinstein, Scarl, and Ulrich, Phys. Rev. 138, B165 (1965).
8. Betz, Arens, Chamberlain, Dost, Grannis, Hansroul, Holloway, Schultz, and Shapiro, Phys. Rev. 148, 1289 (1966).
9. Grannis, Arens, Betz, Chamberlain, Dieterle, Schultz, Shapiro, Steiner, Van Rossum, and Weldon, Phys. Rev. 148, 1297 (1966).
10. Dost, Helmut, University of California Lawrence Radiation Laboratory Report No. UCRL-11877 (unpublished), and Dost, Arens, Betz, Chamberlain, Hansroul, Holloway, Schultz, and Shapiro, Phys. Rev. (to be published) (UCRL-11877 Rev, September 1966).

11. B. M. Golovin, V. P. Dzhelepov, R. Ya. Zul'karneev, and Ts'ui Wa-Ch'uang, J. Exptl. Theoret. Phys. 44, 142 (1963), Soviet Phys. JETP 17, 98 (1963).

12. Atkinson, Cox, Duke, Heard, Jones, Kemp, Murphy, Prentice, and Thresher, Proc. Roy. Soc. A, 289, 449 (1966).

13. Suwa, Yokosawa, Booth, Esterling, and Hill, Phys. Rev. Letters 15, 560 (1965).

14. Yokosawa, Suwa, Hill, Esterling, and Booth, Phys. Rev. Letters 16, 714 (1966).

15. Chamberlain, Hansroul, Johnson, Grannis, Holloway, Valentin, Robrish, and Steiner, Phys. Rev. Letters 17, 975 (1966).

16. S. M. Bilen'kii, Nuovo Cimento 10, 1049 (1958).

17. M. B. Watson, M. Ferro-Luzzi, and R. D. Tripp, Phys. Rev. 131, 2248 (1963).

18. Dieterle, Arens, Chamberlain, Grannis, Hansroul, Holloway, Johnson, Schultz, Shapiro, Steiner, and Weldon, to be published.

19. Chiu, Phillips, and Rarita, Lawrence Radiation Laboratory report UCRL-16940 (1966, unpublished).

20. Dragicescu, Lushchikov, Nikolenko, Taran, and Shapiro, Phys. Letters 12, 334 (1964).

FIGURE CAPTIONS

Fig. 1. Sketch of the apparatus of Abragam et al., that was used to measure the spin correlation coefficient C_{nn} for proton-proton scattering at 20 MeV. A highly polarized proton beam made by alpha-proton scattering is incident on the polarized proton target.

Fig. 2 Plan view of the apparatus of Foot et al., used to measure the polarization P in pion-proton scattering. The pion-proton scattering occurs at the first target. The polarization of the recoiling proton is measured by a second scattering on a carbon target. This technique has for the most part been replaced by polarized-target methods.

Fig. 3. Sketch of the rather simple experimental arrangement of Chamberlain, Jeffries, Schultz, Shapiro, and Van Rossum as used to measure the polarization in pion-proton scattering. The polarized proton target is located at the center of the magnet.

Fig. 4. Elevation view of a more sophisticated apparatus for measuring polarization in elastic scattering. The upper and lower counter arrays each have 10 counters. The beam is incident from the left. The Cherenkov counter C is used for monitoring the beam intensity on the polarized target. To be of interest a scattering event should count in counters U_o, D_d, D_o, one of U_1 to U_{10} and one of D_1 to D_{10}.

Fig. 5. Histogram of coincidence events between the upper counter U_6 and each of the lower counters, D_1 to D_{10}, for the apparatus shown in Fig. 4. The peak in counters D_3 and D_4 represents elastic

scattering on free target protons. The dummy target data show the unwanted contribution from heavy elements in the polarized target. The intensity difference between runs taken with negative and positive target polarization indicates an asymmetry of about 5 percent for this particular scattering process.

Fig. 6. Results of Betz et al. for polarization in proton-proton scattering at 740 MeV lab. kinetic energy. The apparatus has been shown in Fig. 4. The relative systematic error, corresponding to uncertainty in the polarization of the polarized target, is 7 percent. This means there is a 7 percent uncertainty in the scale against which $P(\theta)$ is measured.

Fig. 7. Results of Betz et al. for polarization in proton-proton scattering at 328 MeV, compared to 315-MeV results obtained without benefit of a polarized target.

Fig. 8. Results of Grannis et al. on polarization in proton-proton scattering for incident lab. kinetic energy of 6.15 GeV. The polarization scale is uncertain by 14 percent. t is the invariant square of momentum transfer. θ is the center-of-mass scattering angle.

Fig. 9. Plot of the maximum polarization in proton-proton scattering as a function of lab. kinetic energy T_p.

Fig. 10. Counting rate of scattered pions in a differential range telescope as a function of copper absorber thickness. The solid curve represents data taken with the polarized target in place but not highly polarized. The dashed curve represents dummy target. The difference near 60 grams/cm^2 is due to elastic scattering on free protons in the target.

Fig. 11. Elevation view of the apparatus of Dost et al. for measuring the spin correlation coefficient C_{nn} . The proton beam was polarized by a first scattering on a hydrogen target. The resulting polarized beam was incident on the polarized proton target.

Fig. 12. Results of Dost et al. on C_{nn} in proton-proton scattering at 680 MeV, along with 3 points (open circes) of Golovin et al. at 640 MeV. The Golovin experiment was performed without a polarized proton target.

Fig. 13. Apparatus of Duke et al. for measuring the polarization in pion-proton scattering. A3 and A4 are anticoincidence counters placed against the magnet pole faces.

Fig. 14. Apparatus of Duke et al. as seen from the beam direction. The series of counters B2 , Sp , and Sπ were used to select coplanar scattering events.

Fig. 15. Typical results by Duke et al. The momentum of the incident negative pion beam is 1080 MeV/c. The original scale shows the asymmetry observed. A suitable scale of polarization is indicated by markings at P=0.5 and P= -0.5. The horizontal scale represents the cosine of the center-of-mass scattering angle.

Fig. 16. Polarized target arrangement of Suwa, Yokosawa, Booth, Esterling, and Hill.

Fig. 17. Histogram of coincidence counts between one counter of one bank and each counter of the other bank. The peak near counter 22 is due to elastic pion-proton scattering. The apparatus is shown in Fig. 16.

Fig. 18. Polarization results of Suwa, Yokosawa, Booth, Esterling, and Hill for negative-pion-proton scattering. The momentum of the incident pions was 2.08 GeV/c.

Fig. 19. Elevation view of the apparatus of Hansroul et al. for measuring the polarization in pion-proton scattering. When the incident particles were positive pions it was necessary to use the Cherenkov counter at certain angles of scattering to determine whether the particle reaching the lower set of counters was a pion or a proton.

Fig. 20. Polarization in positive-pion-proton scattering as a function of cosine of center-of-mass scattering angle according to Hansroul et al. The incident beam momentum was 1.441 GeV/c.

Fig. 21. Elevation view of the apparatus of Dieterle et al., used for the K-Σ parity determination. K^+ mesons were detected if they came to rest in the H_2O Cherenkov counter.

Fig. 22. Detail of the apparatus of Dieterle et al. K^+ tange was determined by extrapolation of spark-chamber tracks in the spark chambers K4 and any one of four μ spark chambers placed around the water Cherenkov counter.

Fig. 23. Histogram of "missing mass" for the events of Dieterle et al. obtained with the LMN target. Events on free hydrogen should show as a peak at the sigma mass, but they are here obscured

by a large background due to collisions on heavy elements in the target.

Fig. 24. Histogram of "missing mass" for the events of Dieterle et al. when a CH_2 target was substituted for the LMN target. The peak at the sigma mass indicates the apparatus was adjusted as intended, and allows an estimate to be made of the fraction of LMN events near the sigma mass that are due to free hydrogen.

Fig. 25. Apparatus of the Saclay-Orsay-Pisa collaboration for measuring the polarization in charge-exchange scattering of negative pions on protons. The neutron counters are to the left and right of the beam. A spark chamber was used to detect the gamma rays from the neutral pion.

Fig. 26. The hydrogen peaks, clearly evident above the background (dashed line), of the Saclay-Orsay-Pisa collaboration.

Fig. 27. Polarization results for pion-nucleon charge exchange, from the Saclay-Orsay-Pisa collaboration. t is the square of invariant momentum transfer. P_o is the polarization.

Fig. 28. Plan view of one arrangement used by Borghini et al. to study polarization in pion-proton and proton-proton scattering. K is a Cherenkov counter in the beam used to distinguish pions from protons in the beam. V is an anticoincidence counter. H_2 is a hodoscope used to measure the angle of the scattered beam particle.

Fig. 29. Examples of the hydrogen peaks in the work of Borghini et al.

Fig. 30. Polarization results plotted against invariant square of momentum transfer for pion-proton scattering, from the work of Borghini et al. The curves show predictions of a Regge-pole model.

Fig. 31. Experimental proton-proton polarization results of Borghini et al. (dark circles). The points indicated in the figure as Ref. 5 are Berkeley results. The points indicated as Ref. 6 are probably from the Soviet Union.

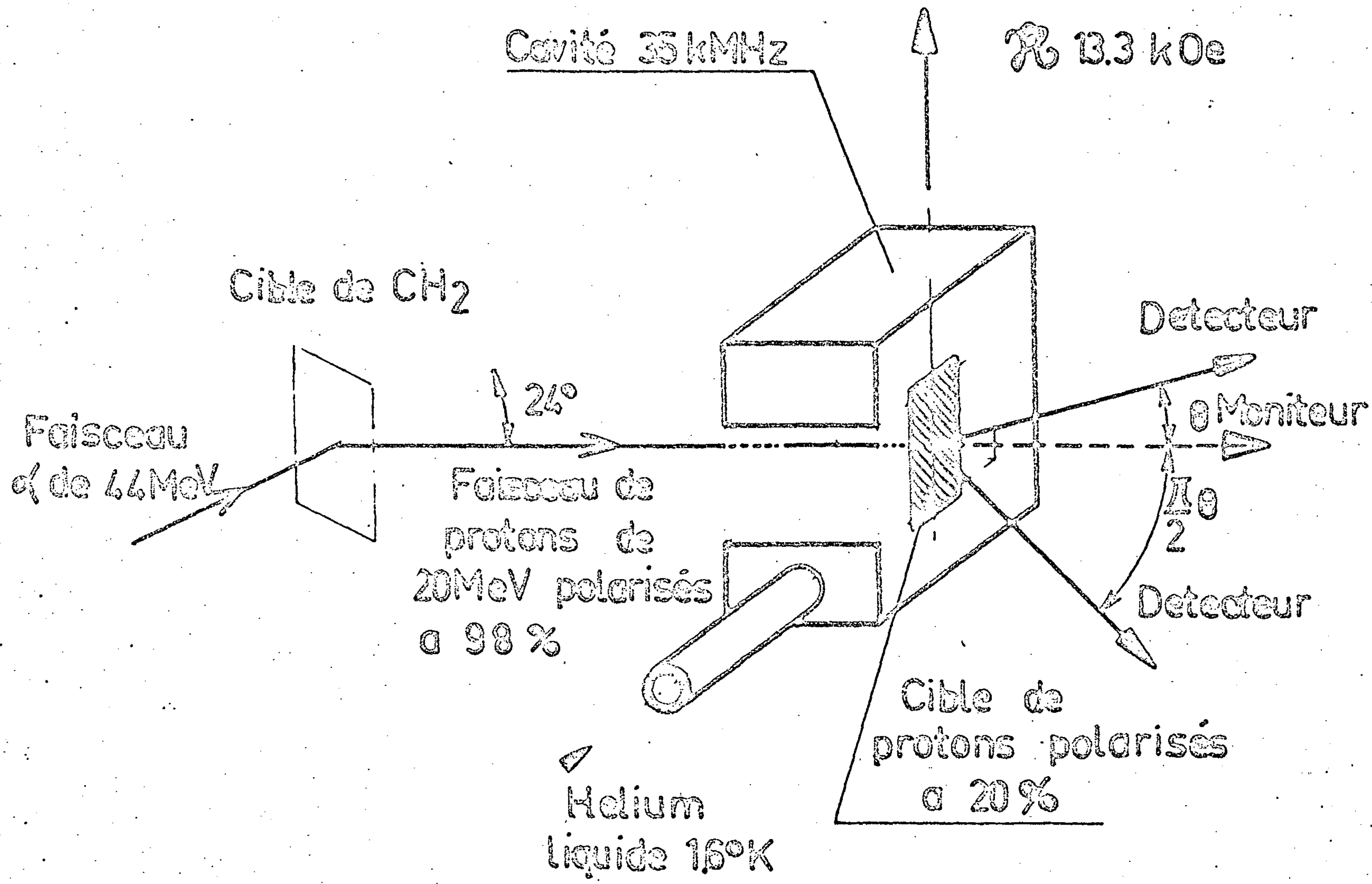

Fig. 1. Schéma général de l'expérience.

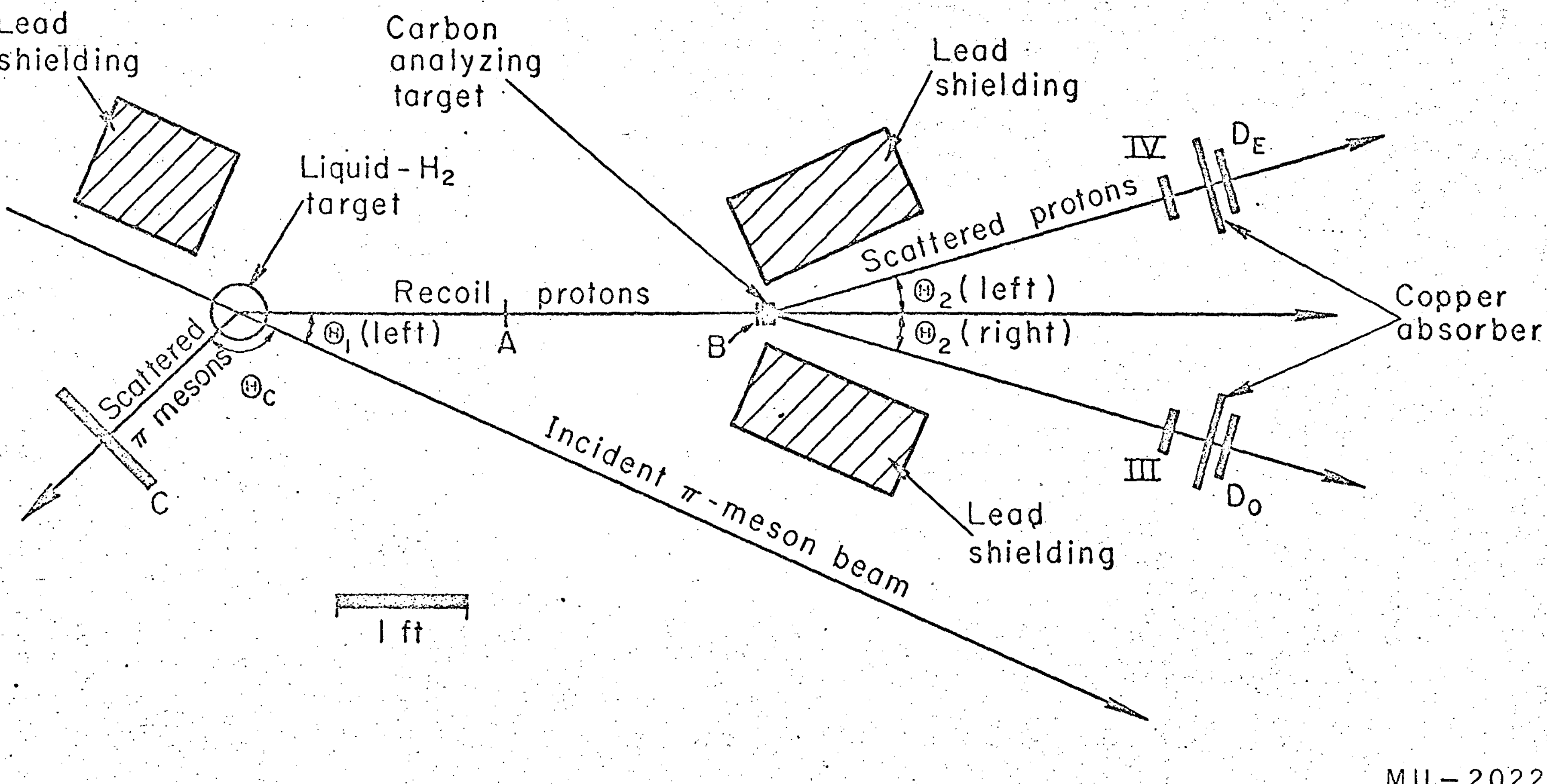
Lead
shielding
Carbon
analyzing
target
Lead
shielding
Liquid - H_2
target
IV
D_E
Scattered protons
Recoil protons
Θ_2 (left)
Θ_2 (right)
Copper
absorber
Θ_1 (left)
A
B
Scattered
π mesons
Θ_c
C
Incident π-meson beam
III
D_0
Lead
shielding
1 ft
MU-20228

Fig. 2

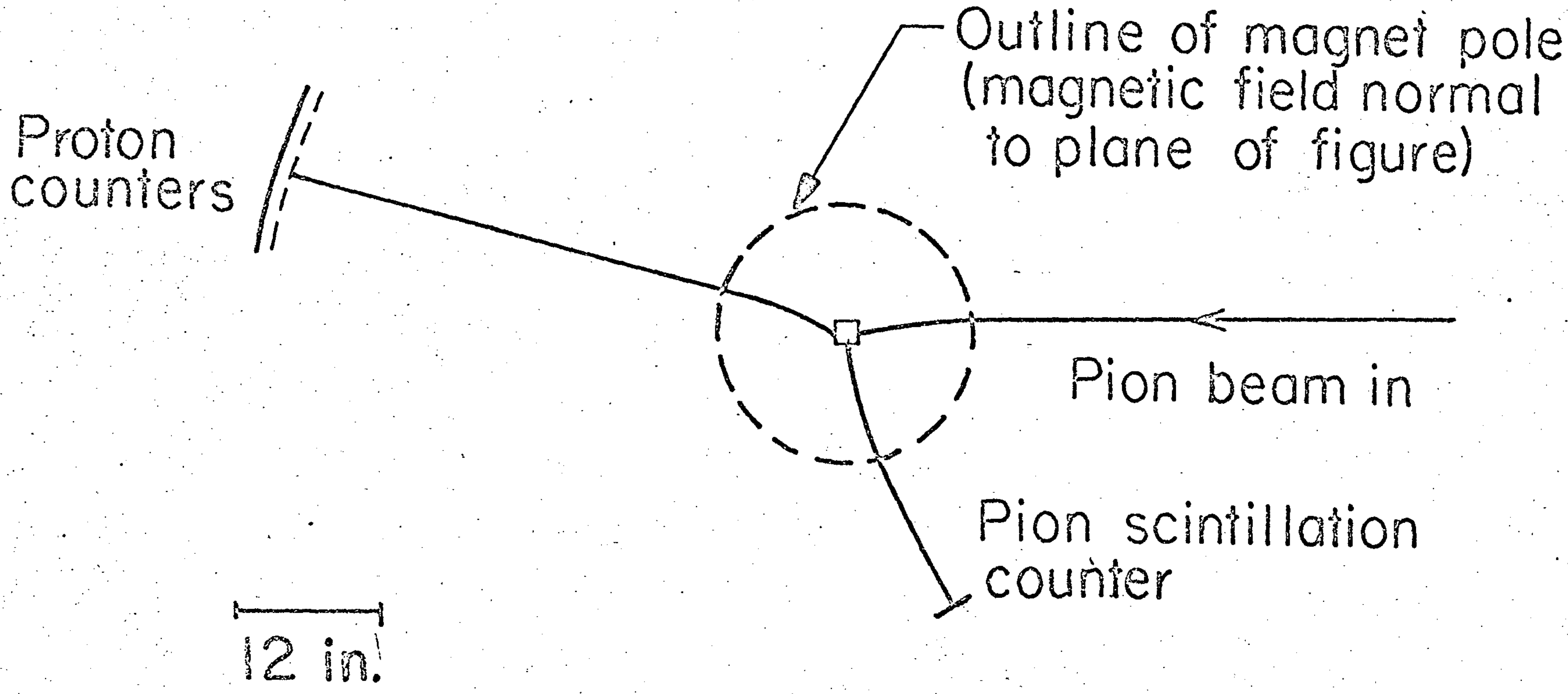

MU-30598A

Fig. 3

UCRL-7433

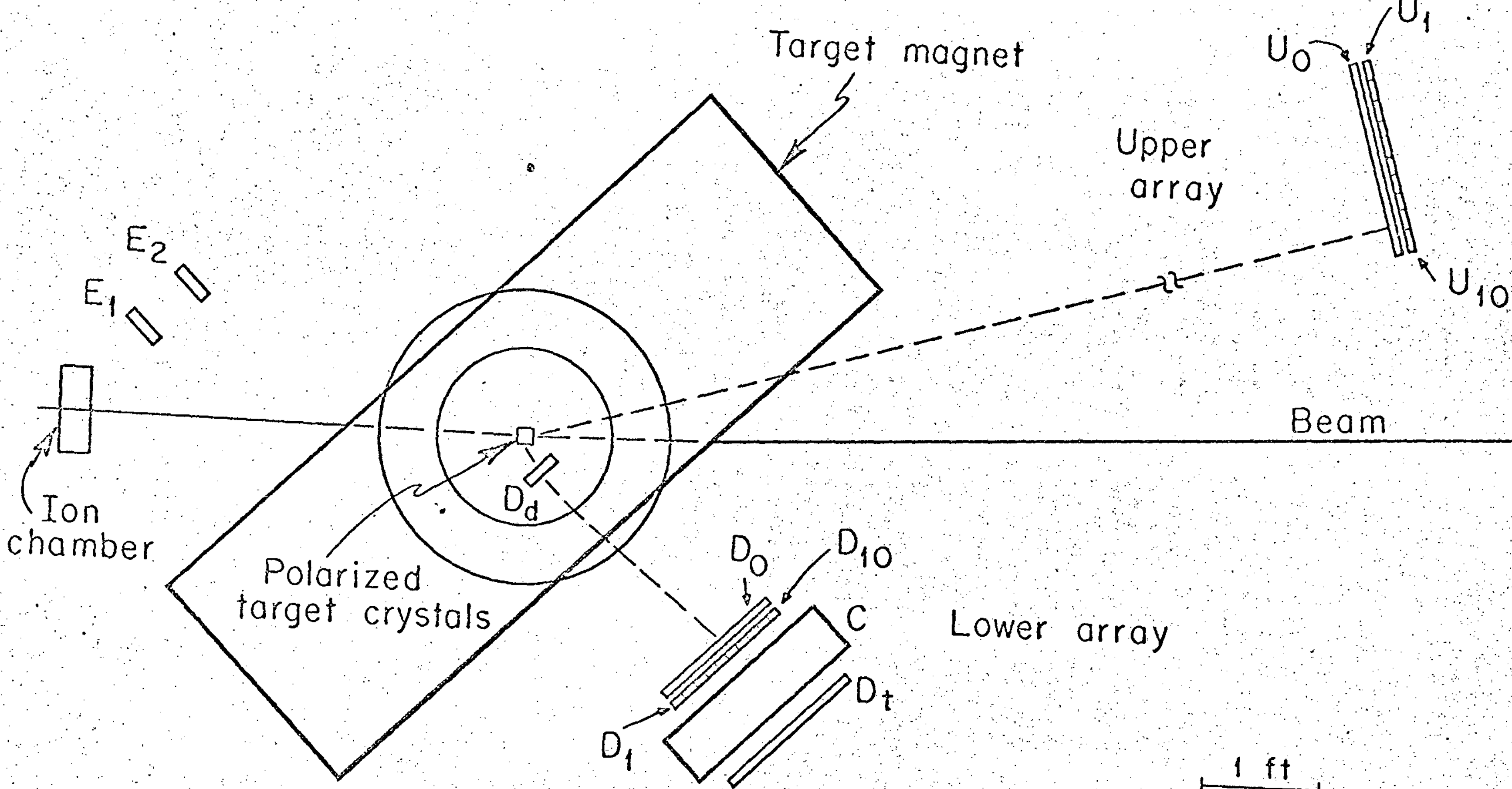

Fig. 4

MU-35856

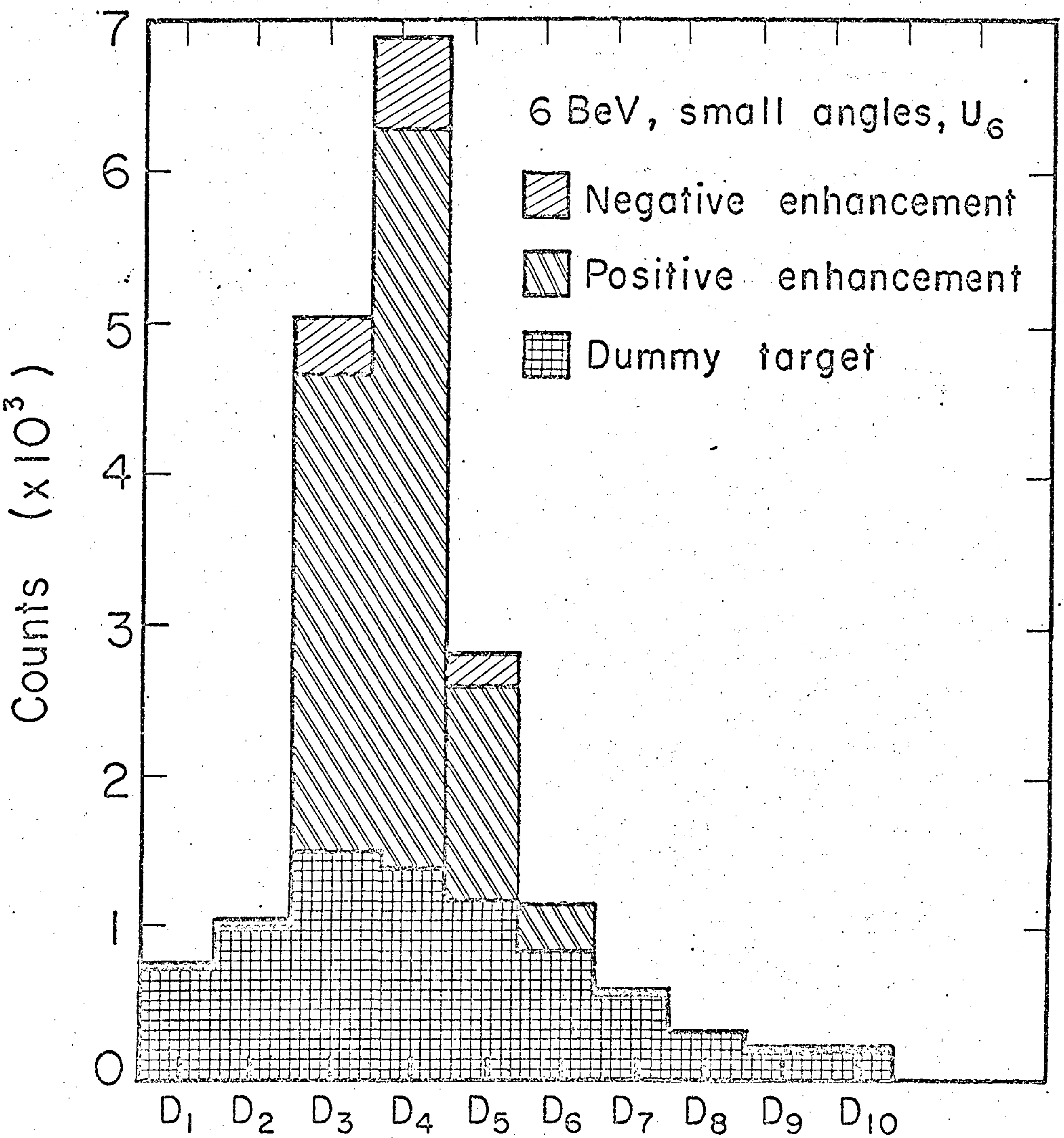

MU-33098

Fig. 5

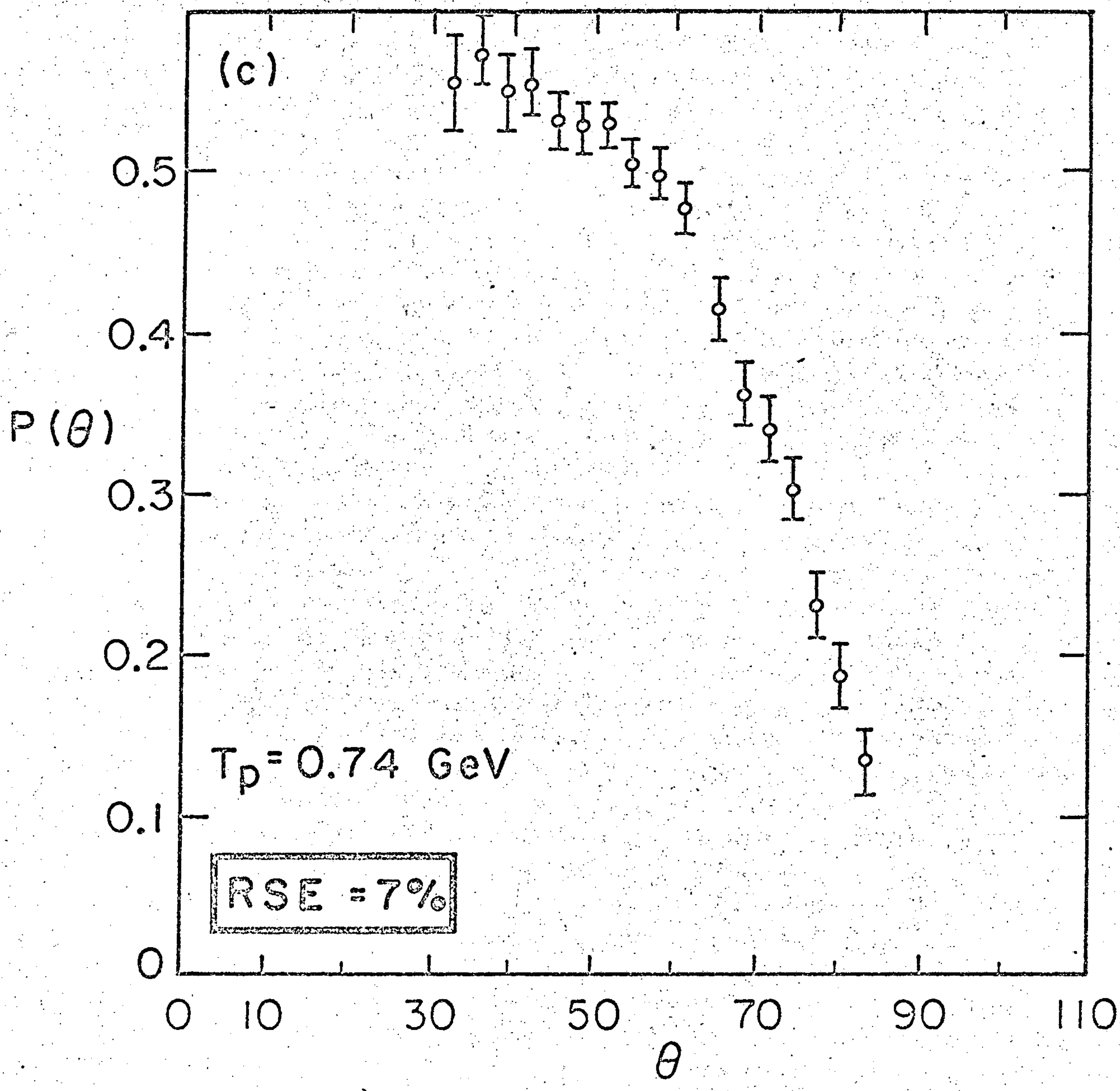

MUB-3464

Fig. 6

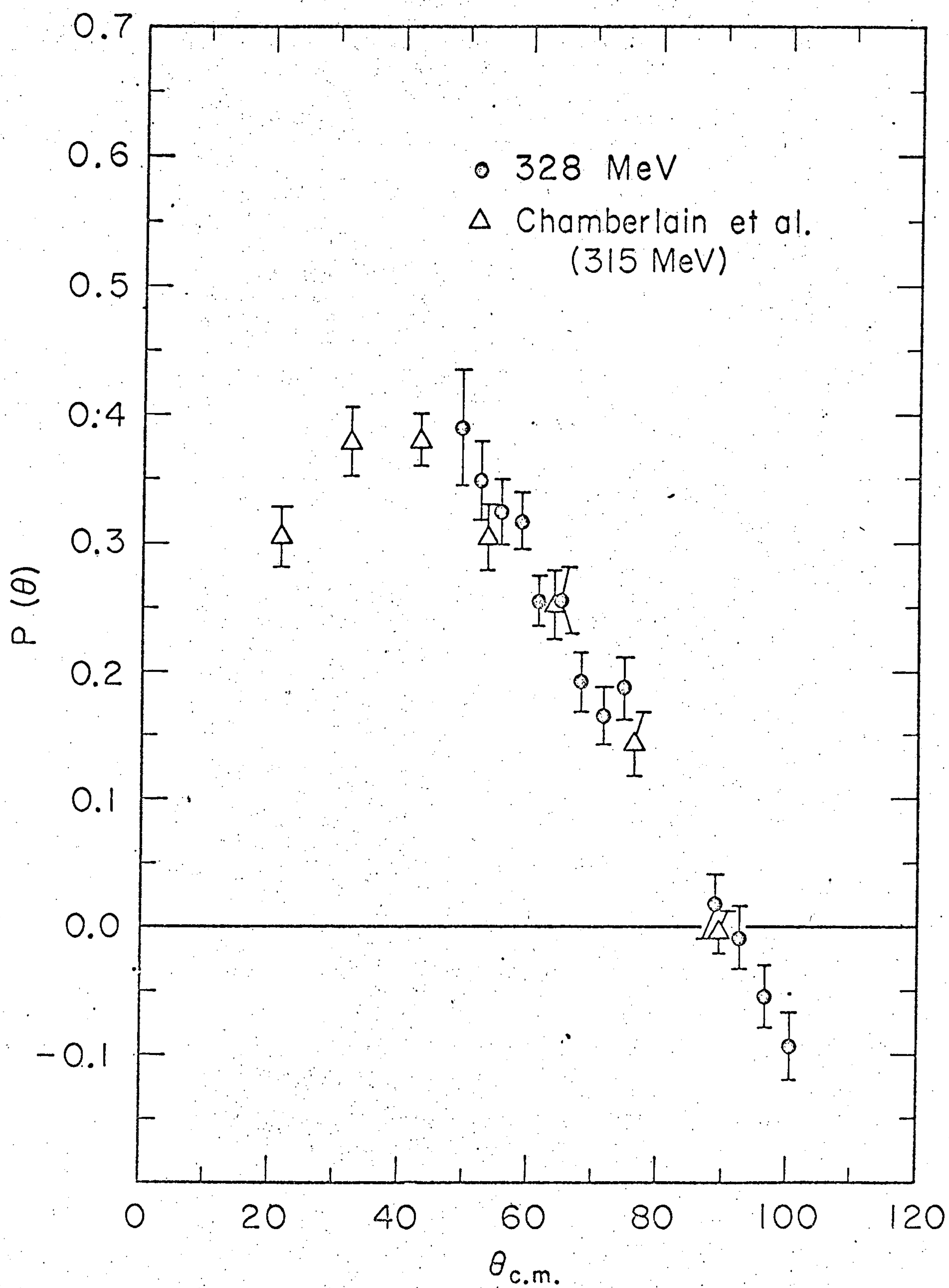

Fig. 7

MU-34598

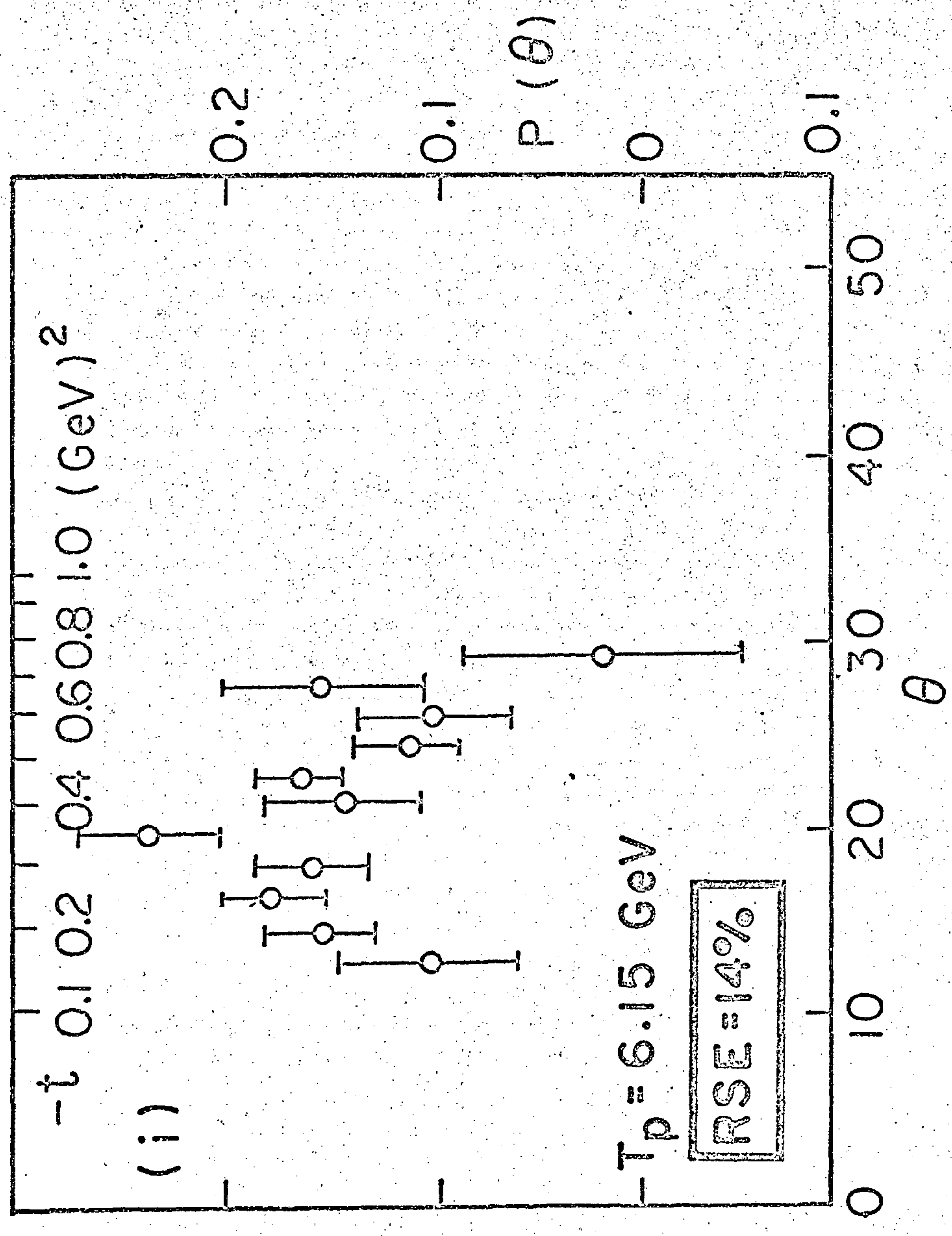

MUB-3470

Fig. 8

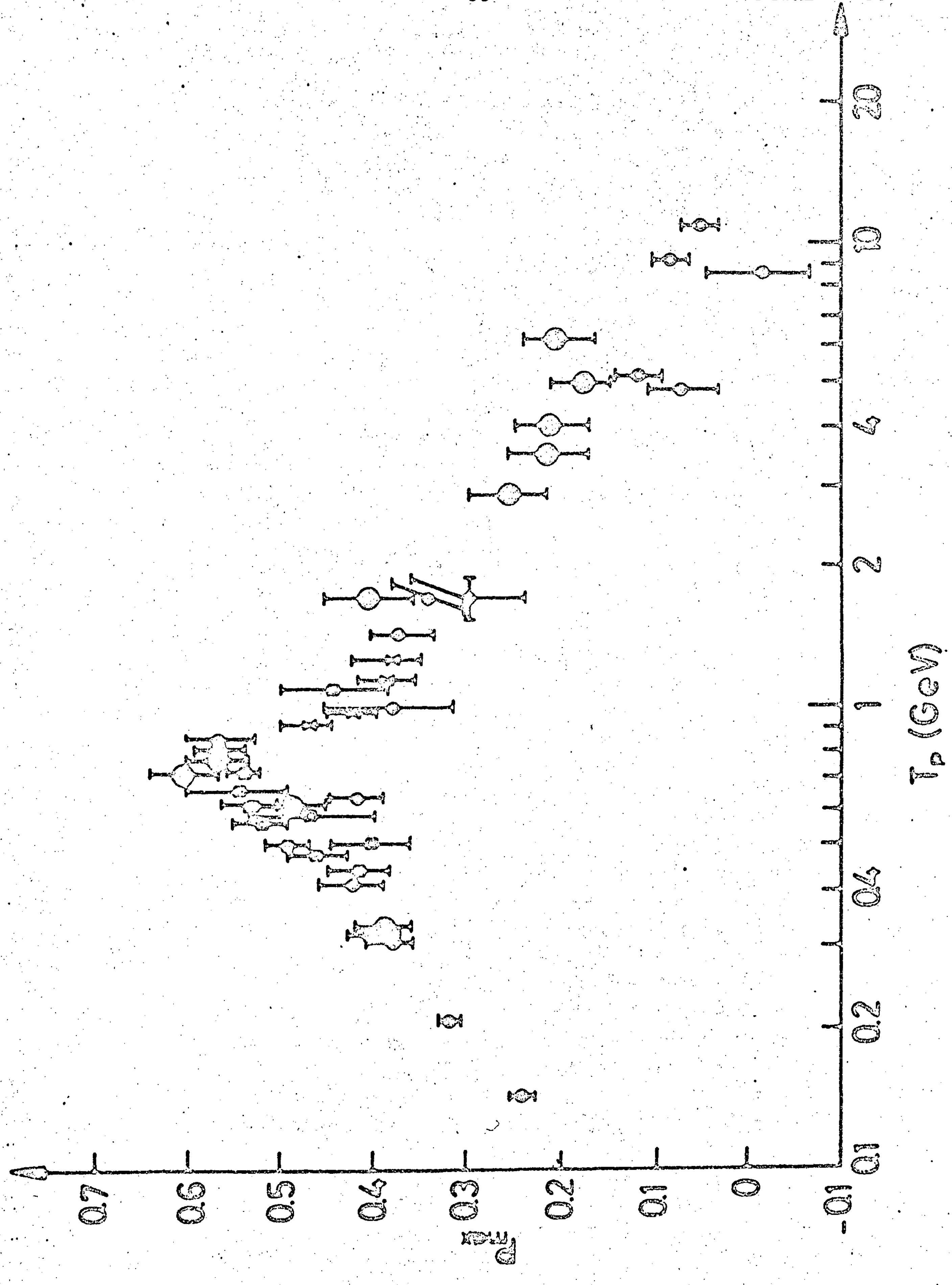

Fig. 9

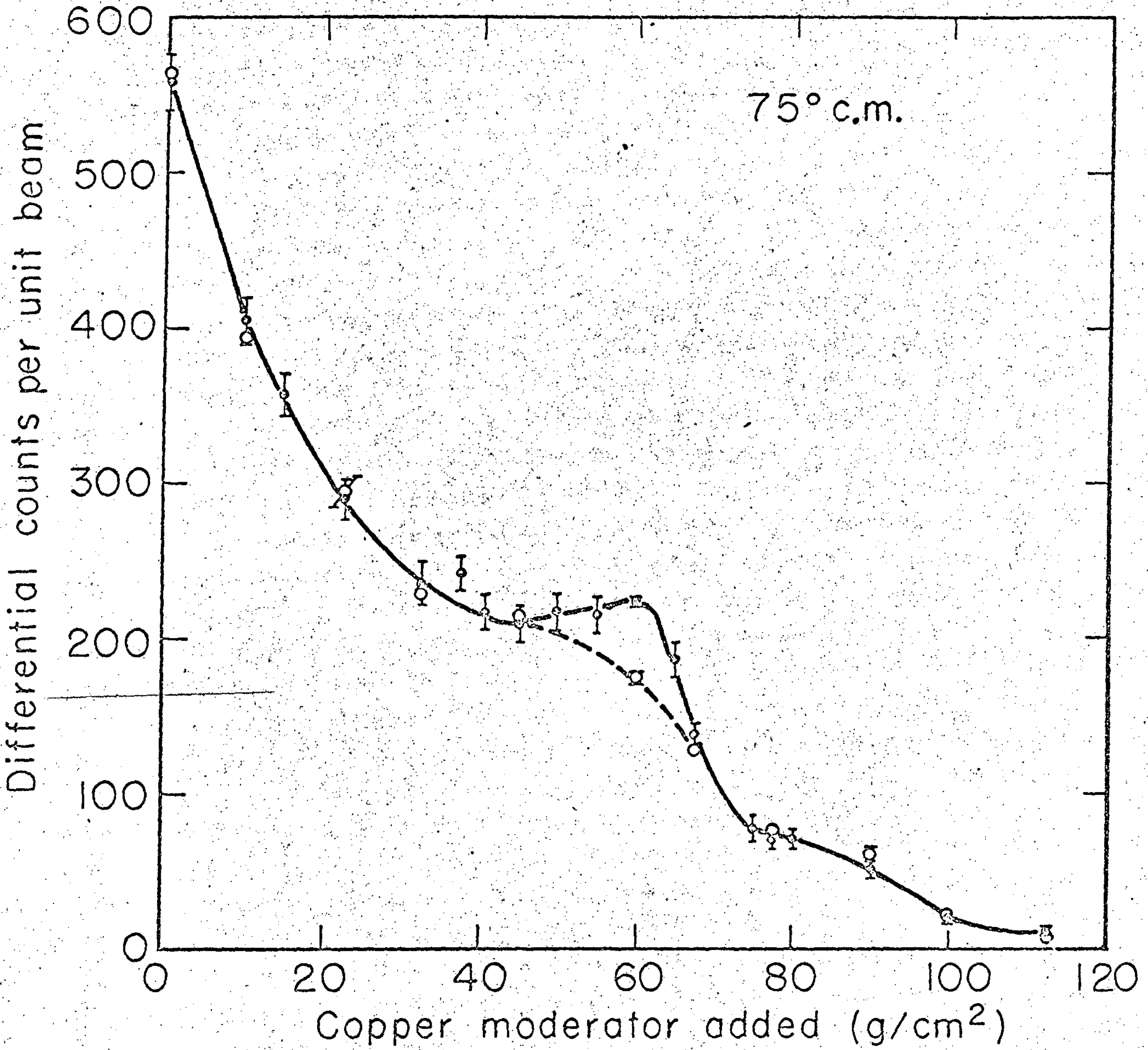

Fig. 10

MU-29815

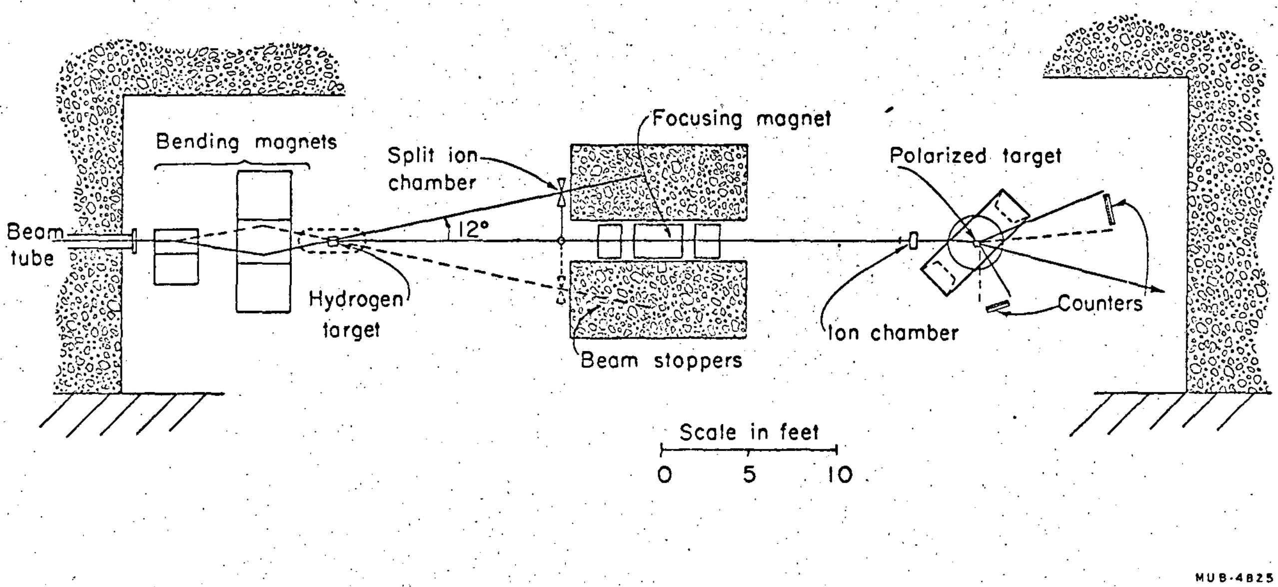
Bending magnets
Split ion chamber
Focusing magnet
Polarized target
Beam tube
12°
Hydrogen target
Beam stoppers
Ion chamber
Counters
Scale in feet
0 5 10
MUB-4825

Fig. 11

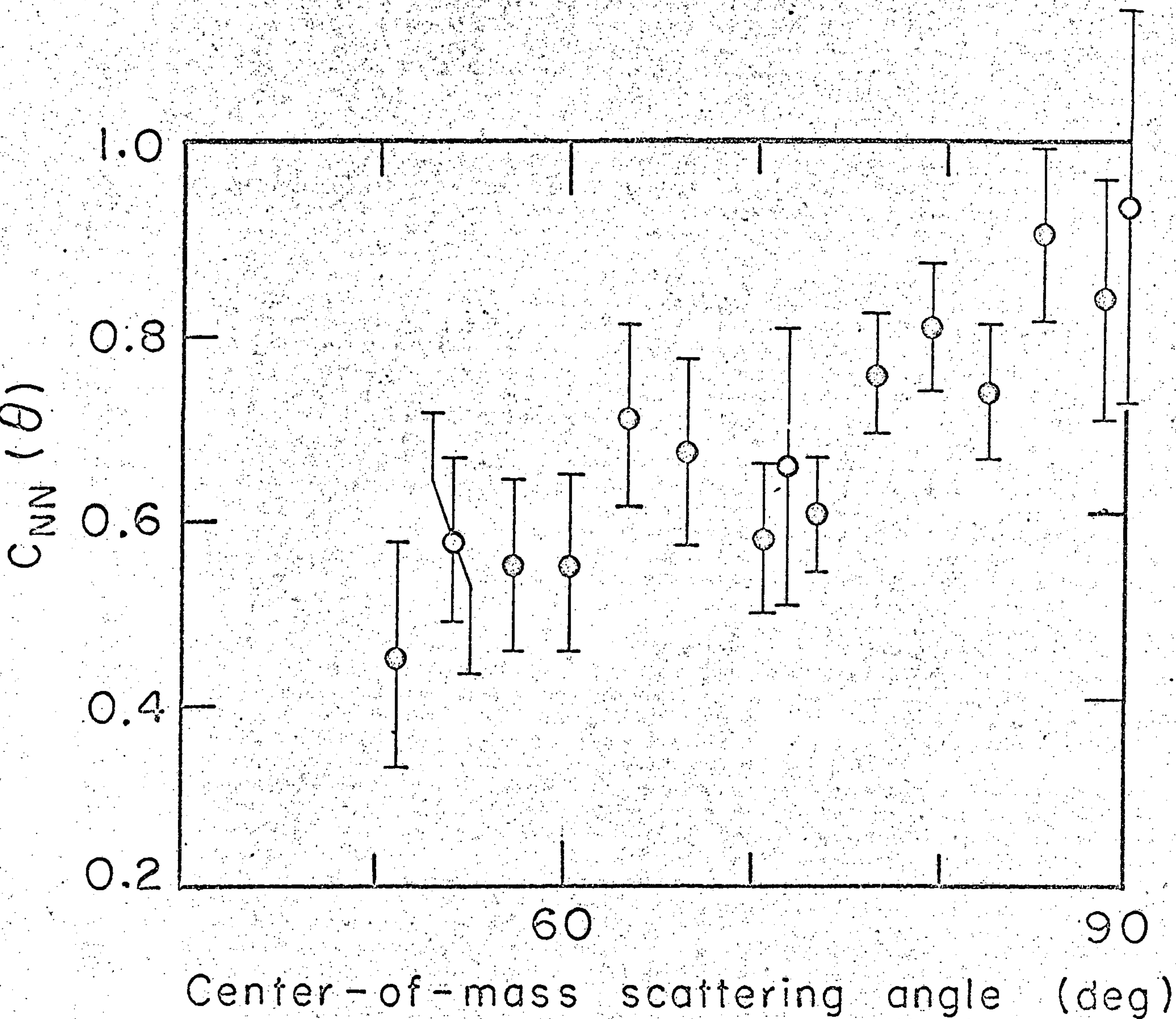

Fig. 12 MU-35185

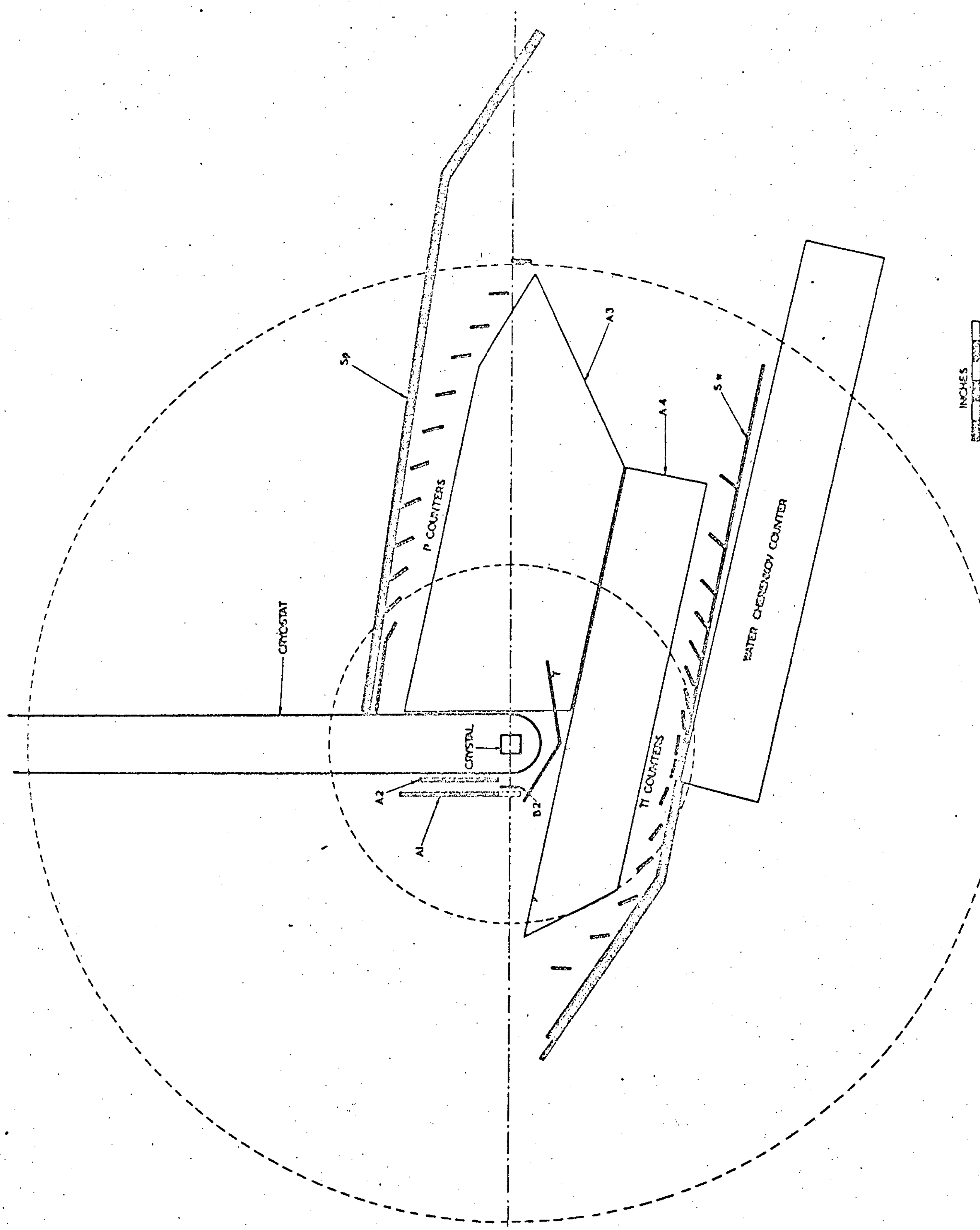
CRYOSTAT
CRYSTAL
P COUNTERS
π COUNTERS
WATER CHERENKOV COUNTER
A1
A2
A3
A4
B2
INCHES

Fig. 13

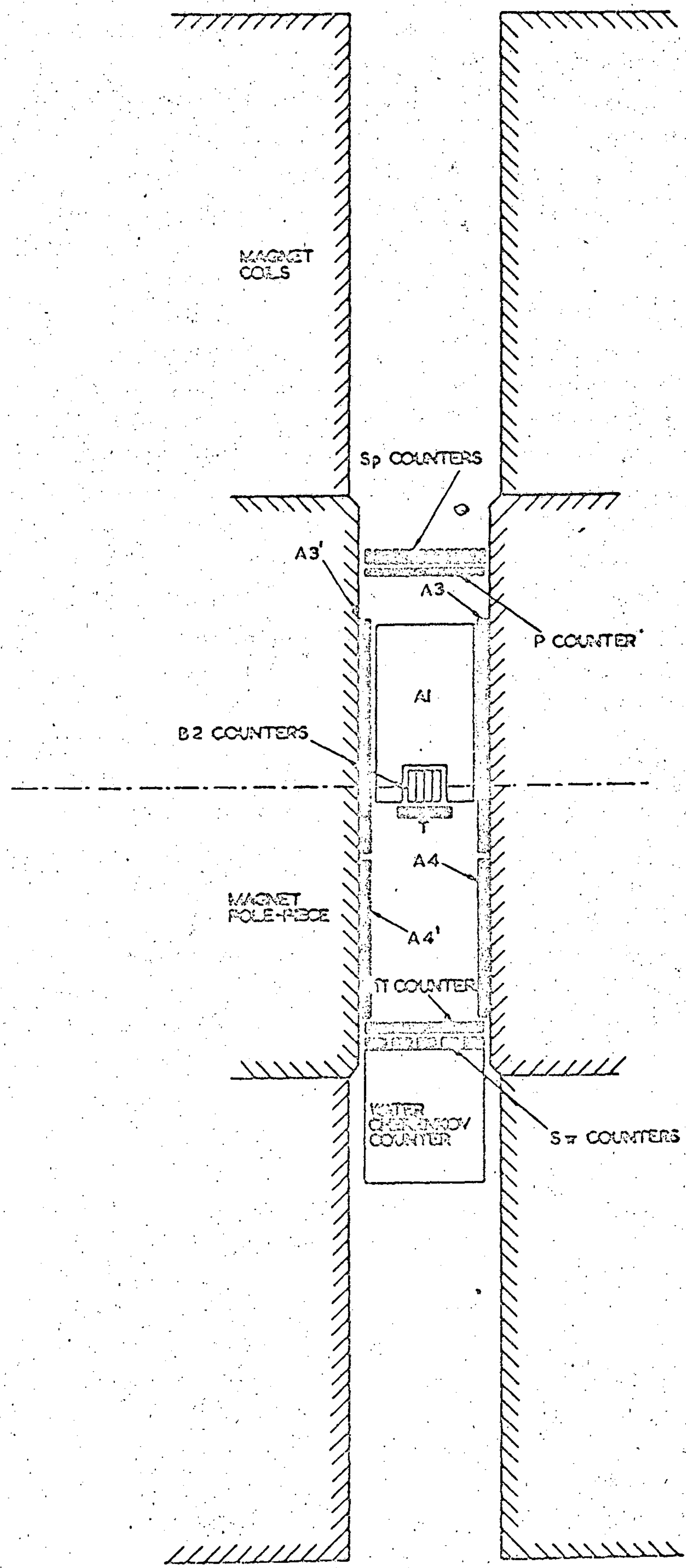
MAGNET COILS
Sp COUNTERS
A3'
A3
P COUNTER
Al
B2 COUNTERS
T
A4
MAGNET POLE-PIECE
A4'
π COUNTER
WATER CHERENKOV COUNTER
Sπ COUNTERS

Fig. 14

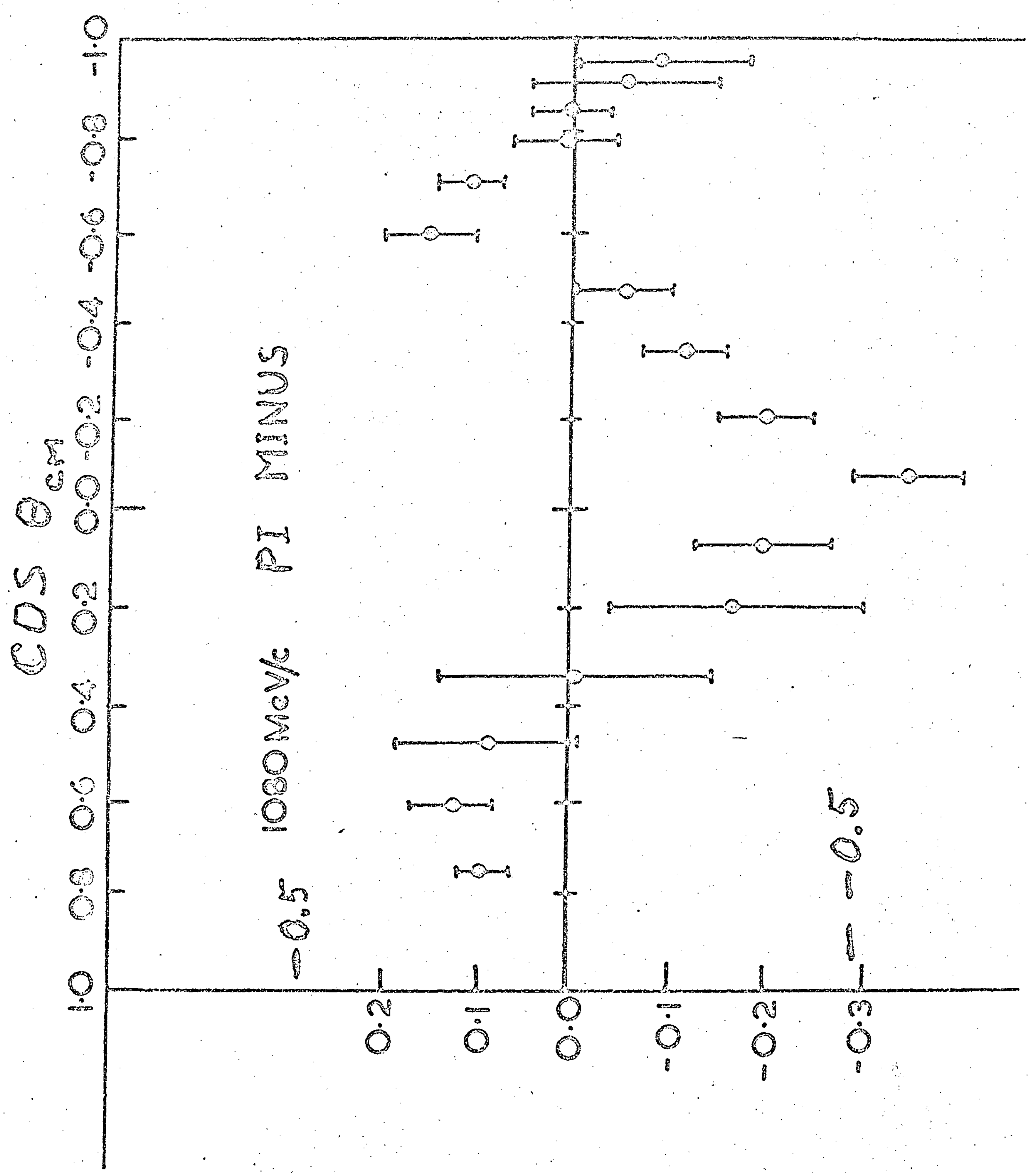
COS θcm
PI MINUS
1080 MeV/c
-0.5
-0.5
1.0 0.8 0.6 0.4 0.2 0.0 -0.2 -0.4 -0.6 -0.8 -1.0
0.2 0.1 0.0 -0.1 -0.2 -0.3

Fig. 15

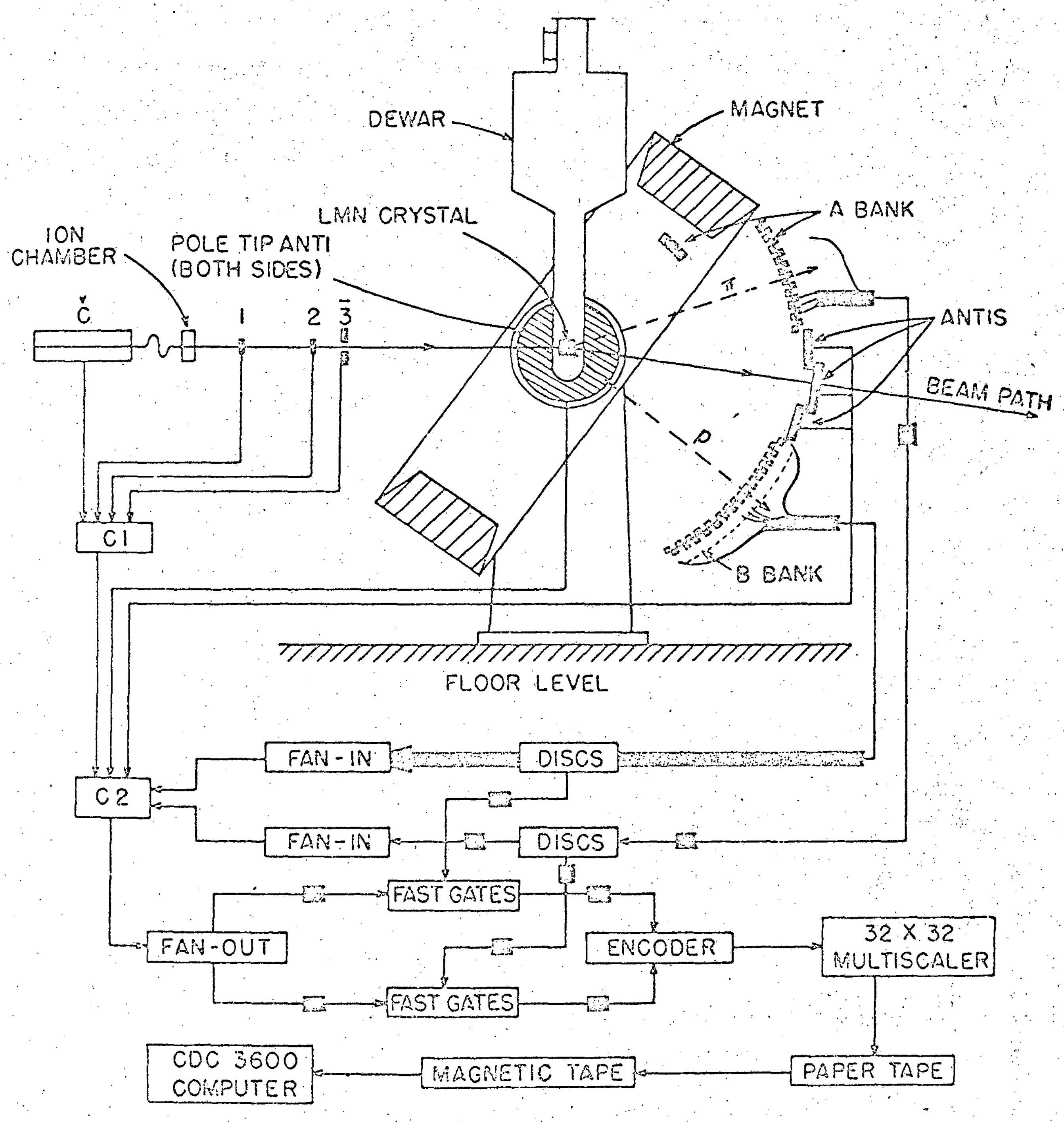
DEWAR
MAGNET
LMN CRYSTAL
A BANK
ION CHAMBER
POLE TIP ANTI (BOTH SIDES)
C
1
2
3
ANTIS
BEAM PATH
B BANK
C1
FLOOR LEVEL
FAN-IN
DISCS
C2
FAN-IN
DISCS
FAST GATES
FAN-OUT
ENCODER
32 X 32 MULTISCALER
FAST GATES
CDC 3600 COMPUTER
MAGNETIC TAPE
PAPER TAPE

Fig. 16

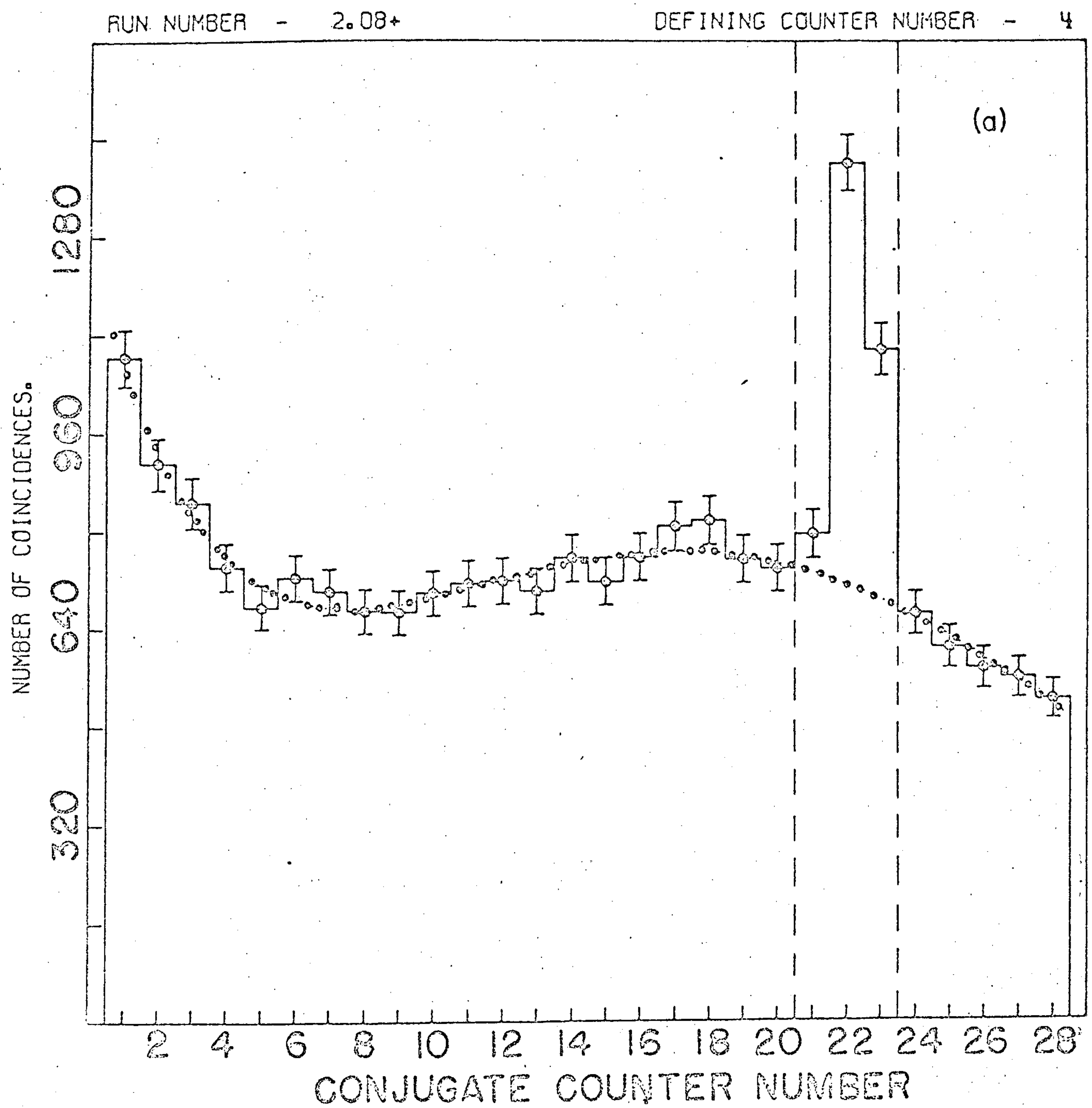
RUN NUMBER - 2.08+
DEFINING COUNTER NUMBER - 4
(a)
NUMBER OF COINCIDENCES.
320
640
960
1280
2 4 6 8 10 12 14 16 18 20 22 24 26 28
CONJUGATE COUNTER NUMBER

Fig. 17

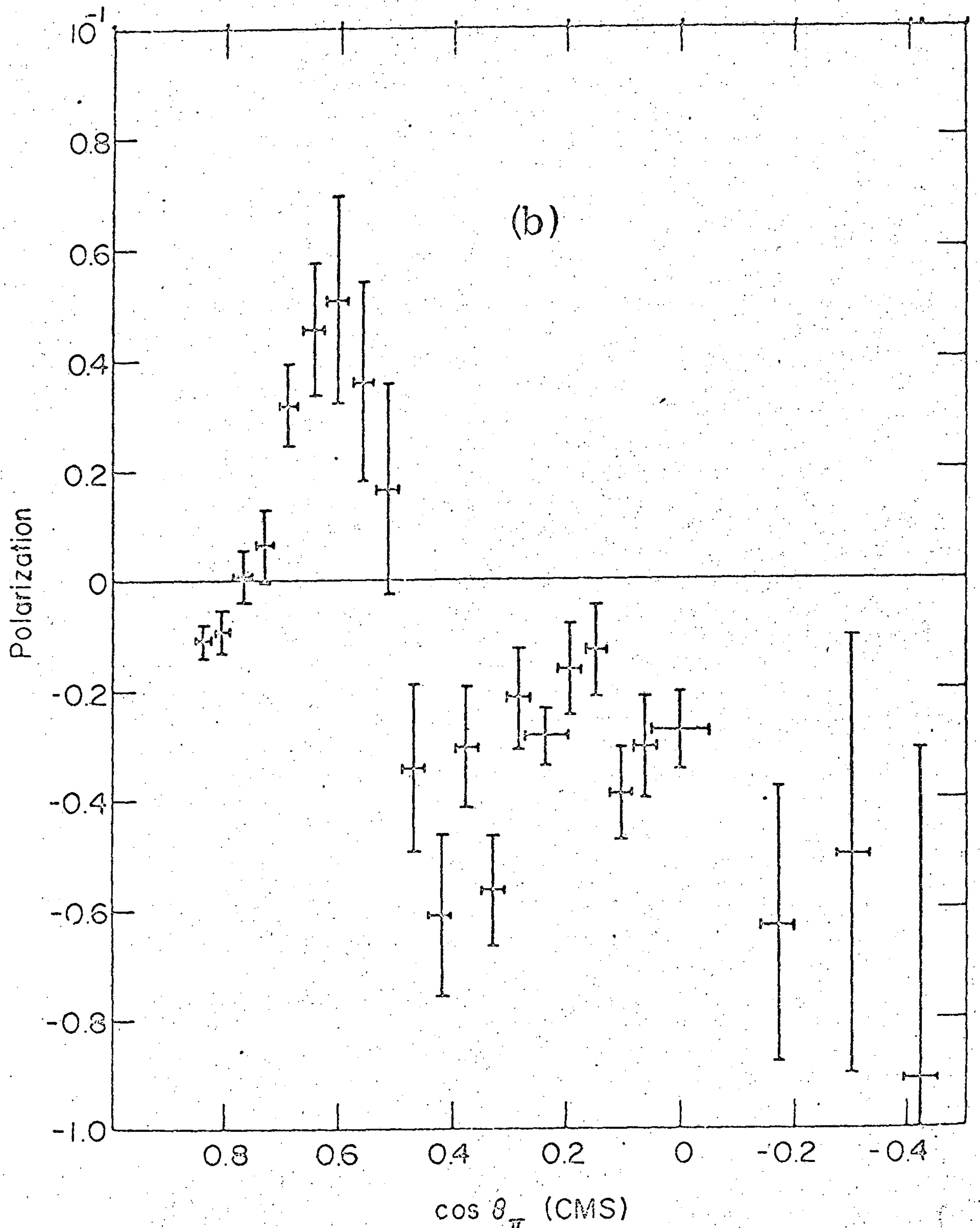
(b)
Polarization
cos θ_π (CMS)
10^{-1}
0.8
0.6
0.4
0.2
0
-0.2
-0.4
-0.6
-0.8
-1.0
0.8
0.6
0.4
0.2
0
-0.2
-0.4

Fig. 18

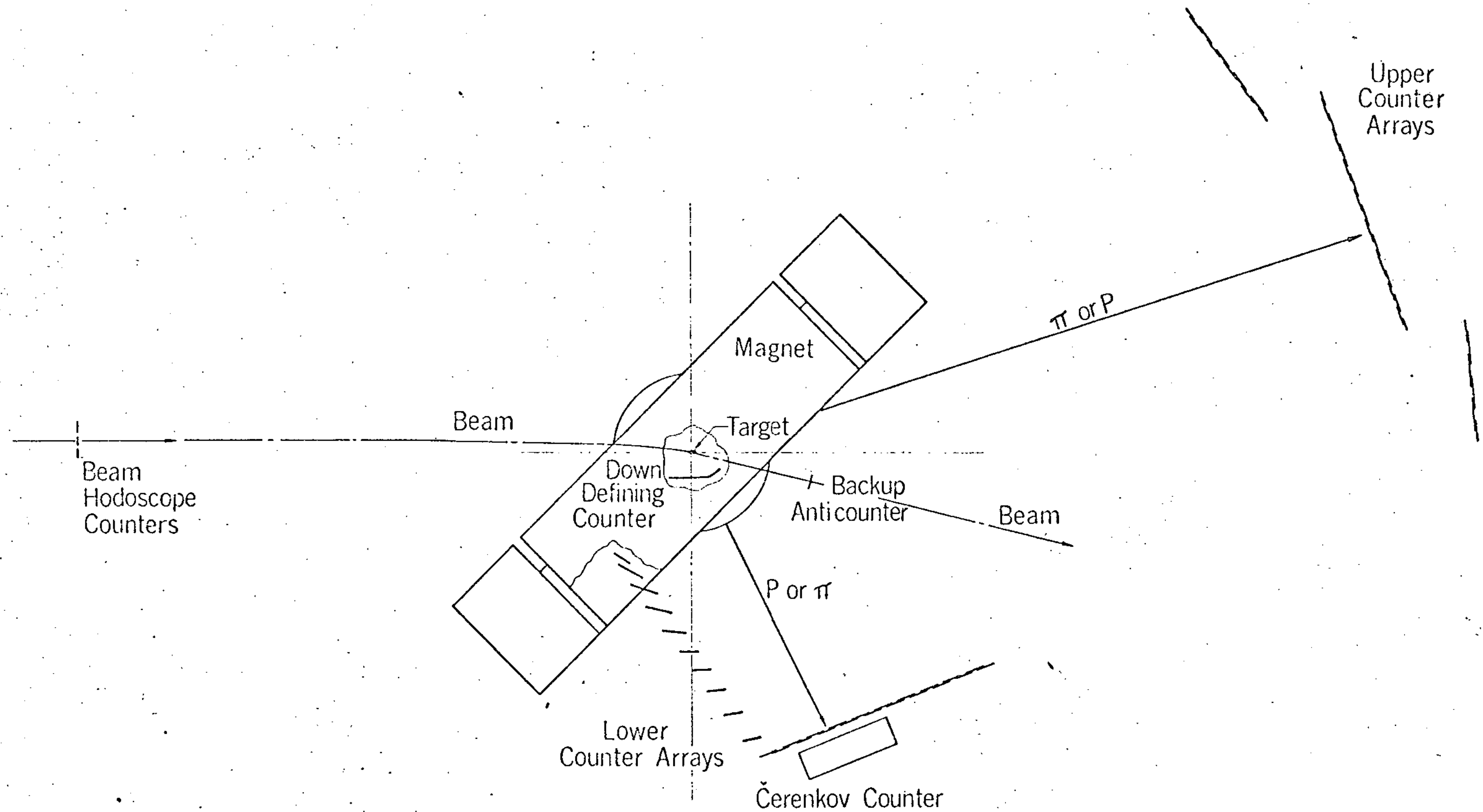

EXPERIMENTAL ARRANGEMENT

Fig. 19

MUB-9346

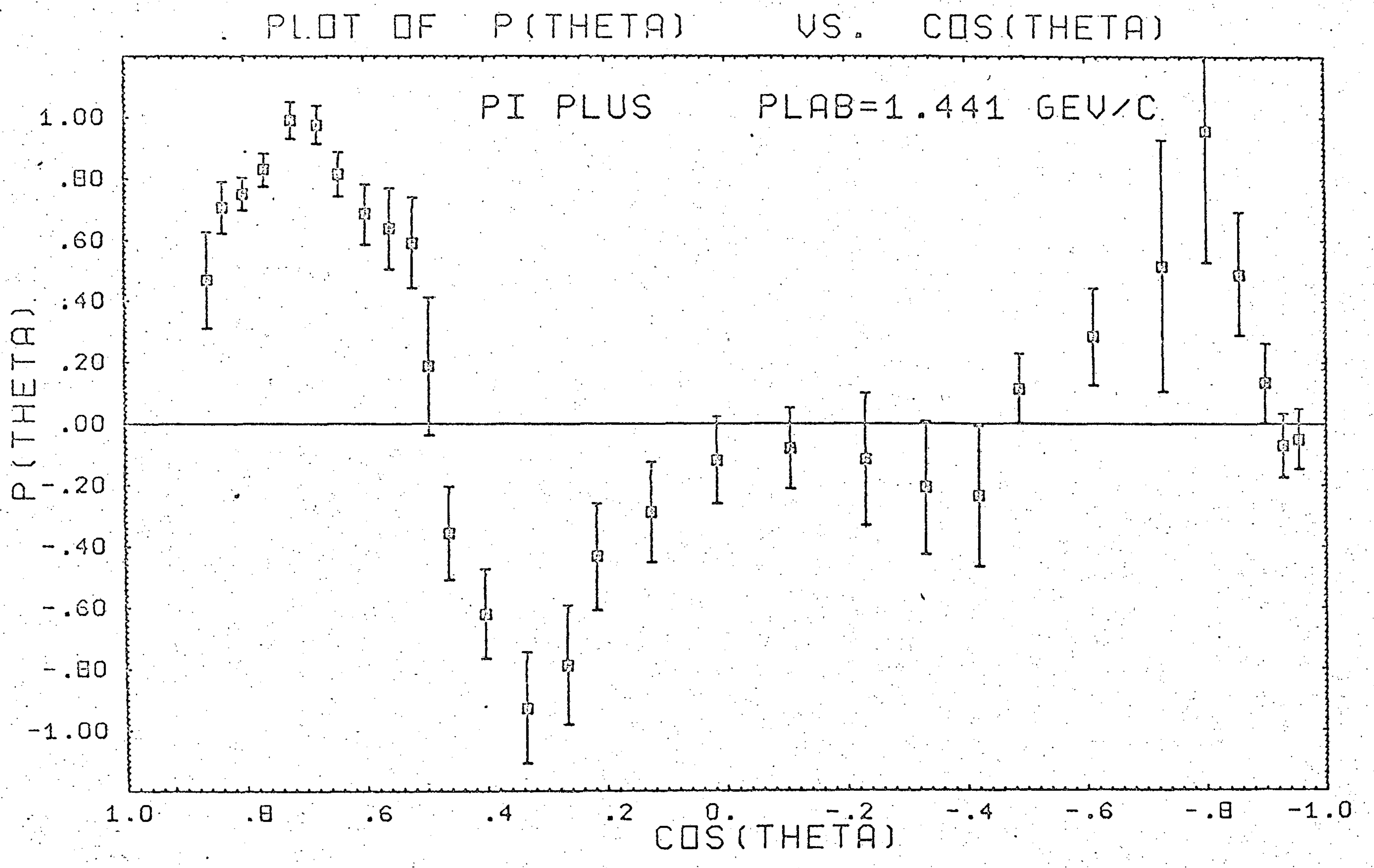
PLOT OF P(THETA) VS. COS(THETA)
PI PLUS PLAB=1.441 GEV/C
P(THETA)
1.00
.80
.60
.40
.20
.00
-.20
-.40
-.60
-.80
-1.00
1.0
.8
.6
.4
.2
0.
-.2
-.4
-.6
-.8
-1.0
COS(THETA)

Fig. 20

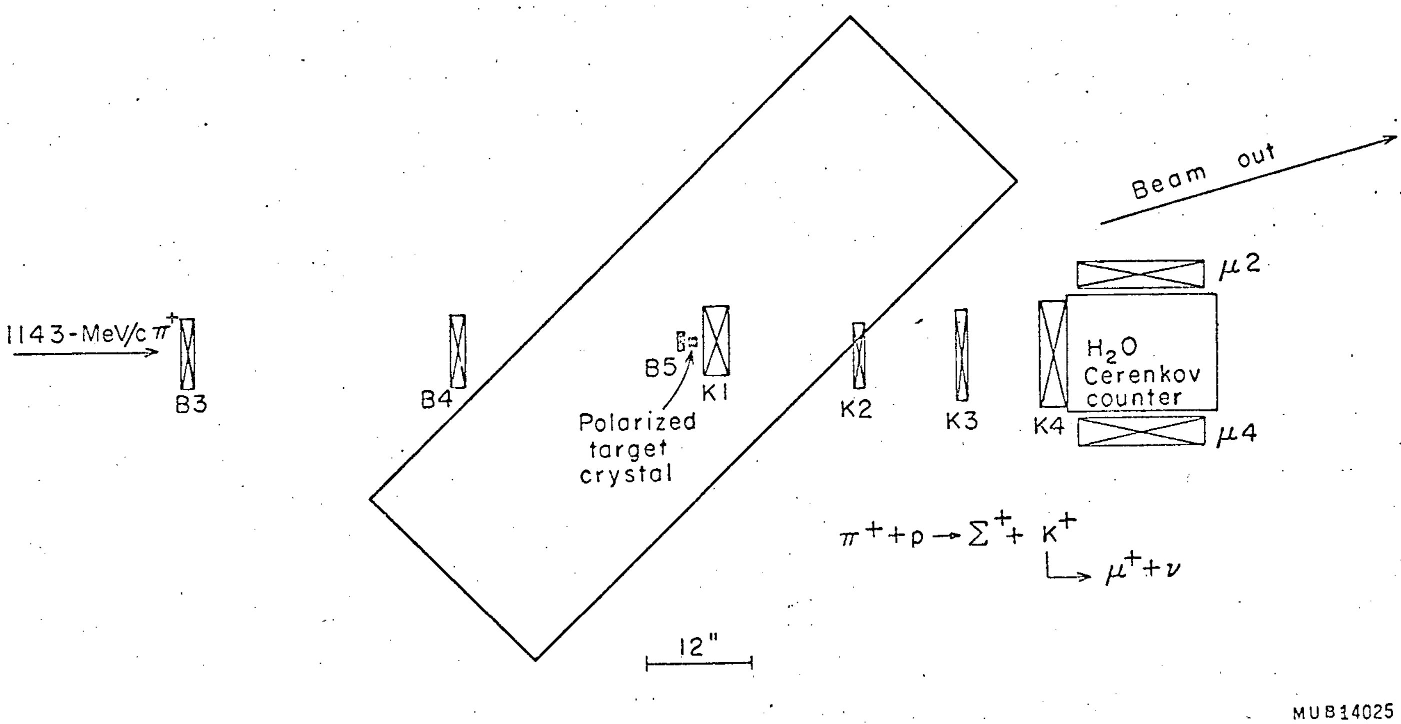
Beam out
1143-MeV/c π^+
B3
B4
B5
Polarized target crystal
K1
K2
K3
K4
$\mu 2$
H_2O Cerenkov counter
$\mu 4$
$\pi^+ + p \rightarrow \Sigma^+ + K^+$
$\hookrightarrow \mu^+ + \nu$
12"
MUB14025

Fig. 21

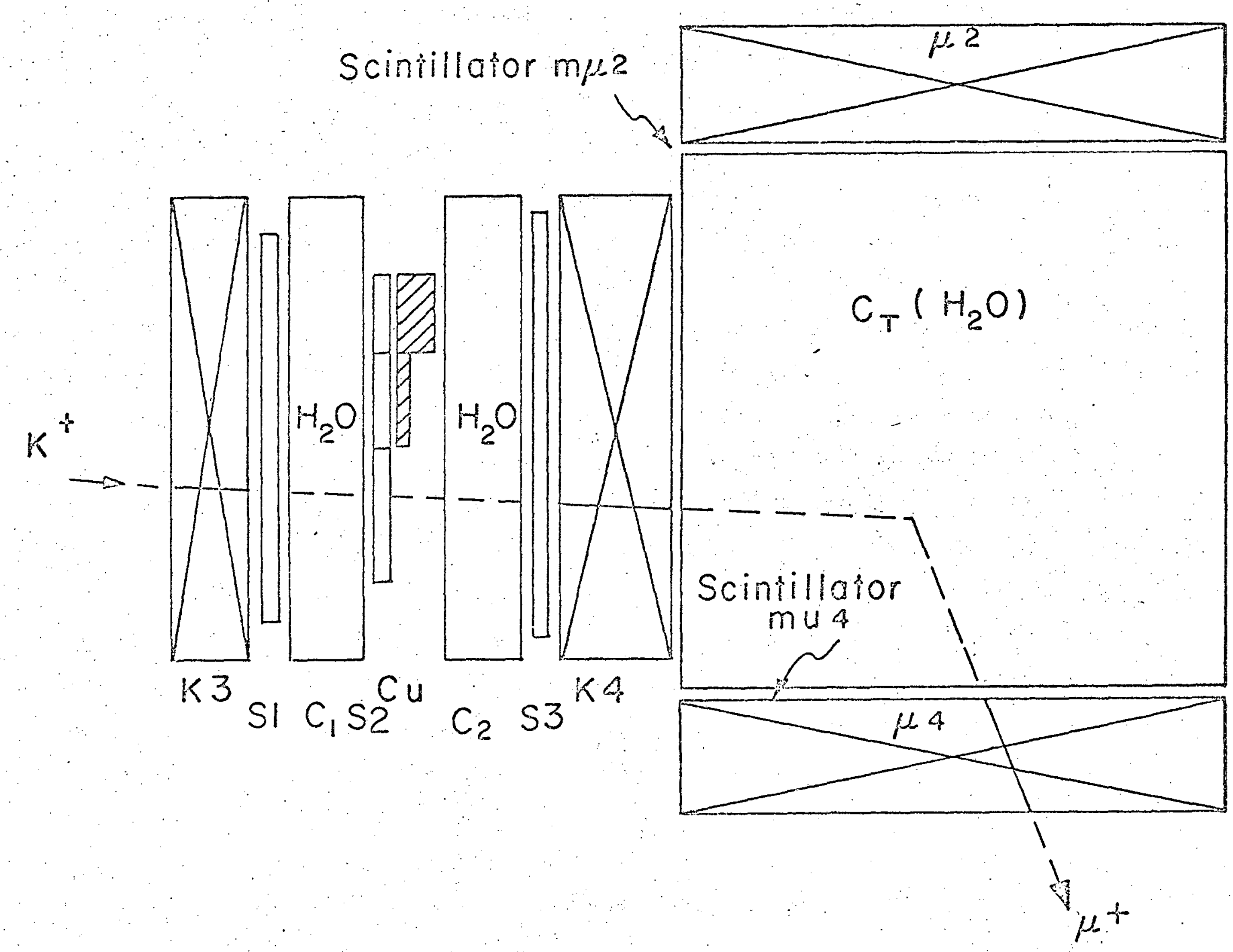

MUB-13891

Fig. 22

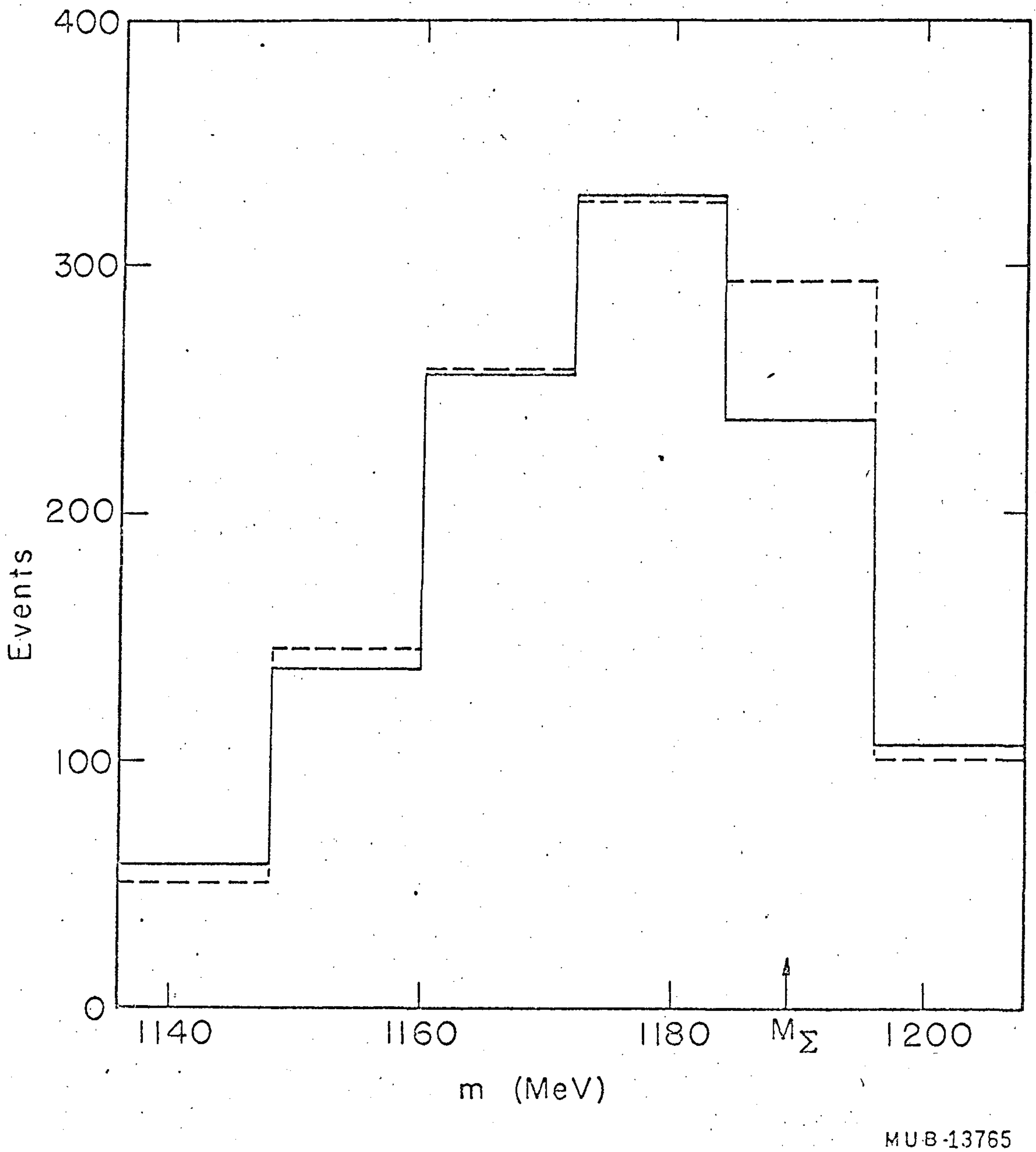
400
300
200
100
0
Events
1140
1160
1180
M_Σ
1200
m (MeV)
MUB-13765

Fig. 23

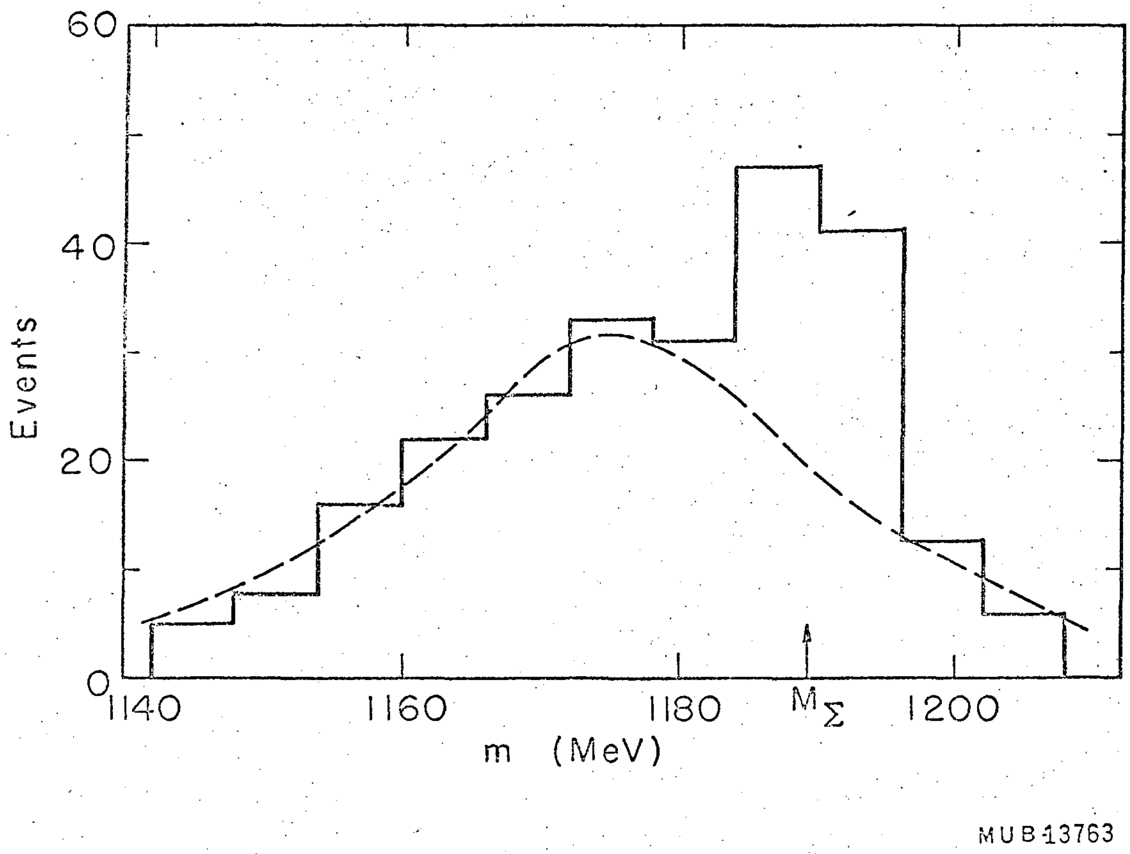

Fig. 24

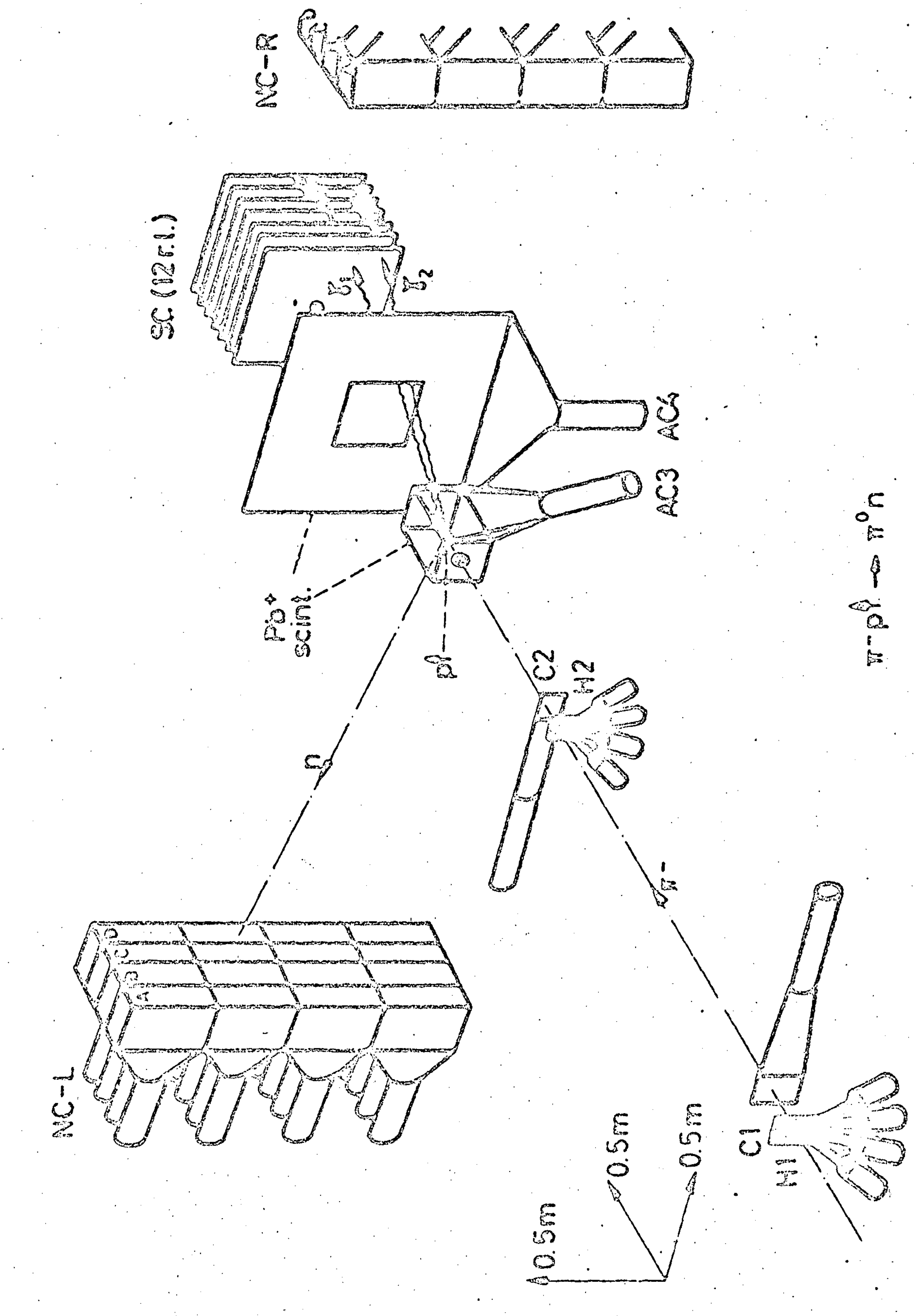
NC-R
SC (12 r.l.)
γ_1
γ_2
AC4
AC3
Pb + scint.
$p^{\uparrow}$
C2
H2
n
π^-
NC-L
A B C D
C1
H1
0.5m
0.5m
0.5m
$\pi^- p^{\uparrow} \to \pi^0 n$

Fig. 25

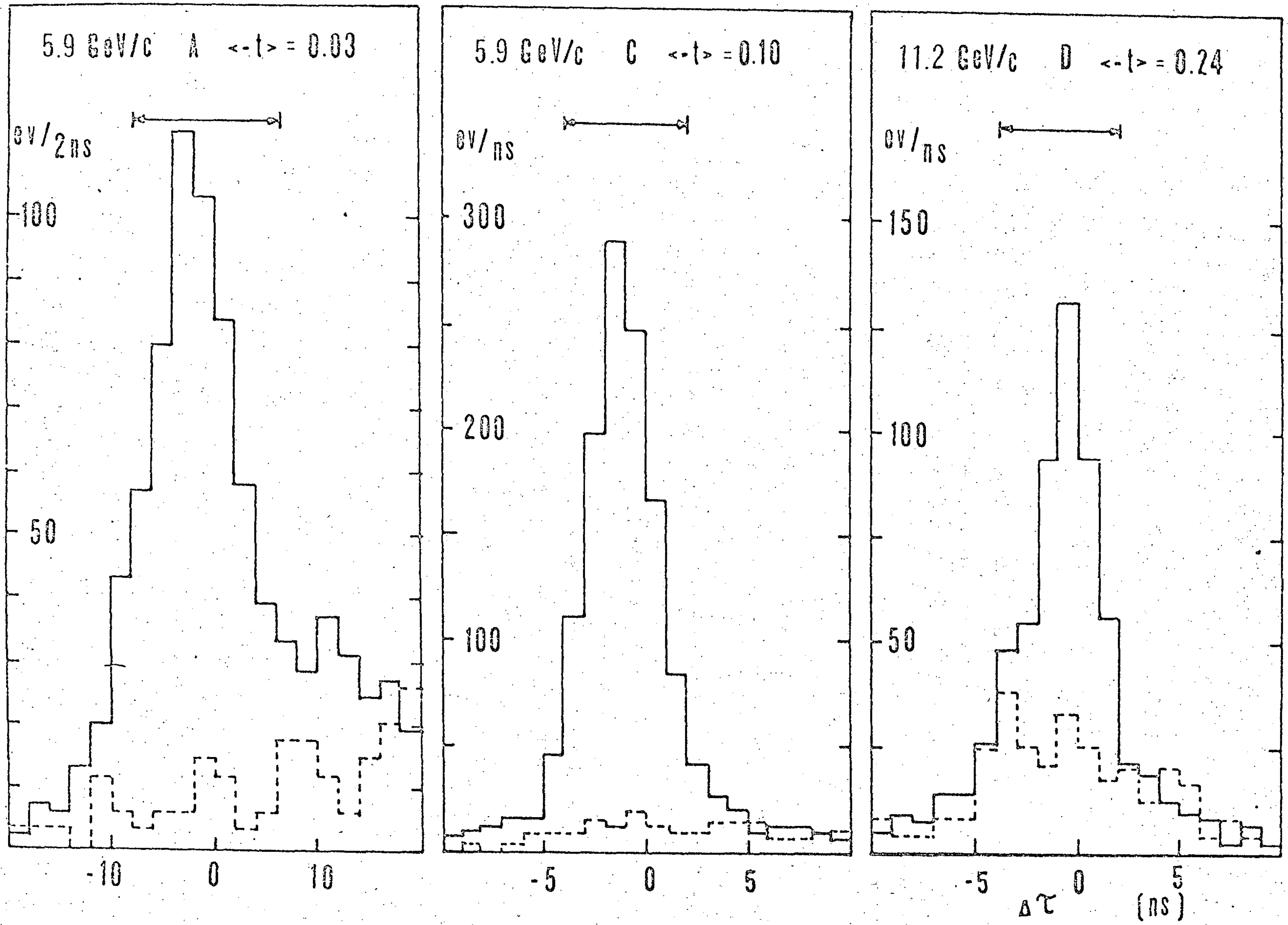
5.9 GeV/c A <-t> = 0.03
ev/2ns
100
50
-10
0
10
5.9 GeV/c C <-t> = 0.10
ev/ns
300
200
100
-5
0
5
11.2 GeV/c D <-t> = 0.24
ev/ns
150
100
50
-5
0
5
Δτ
(ns)

Fig. 26

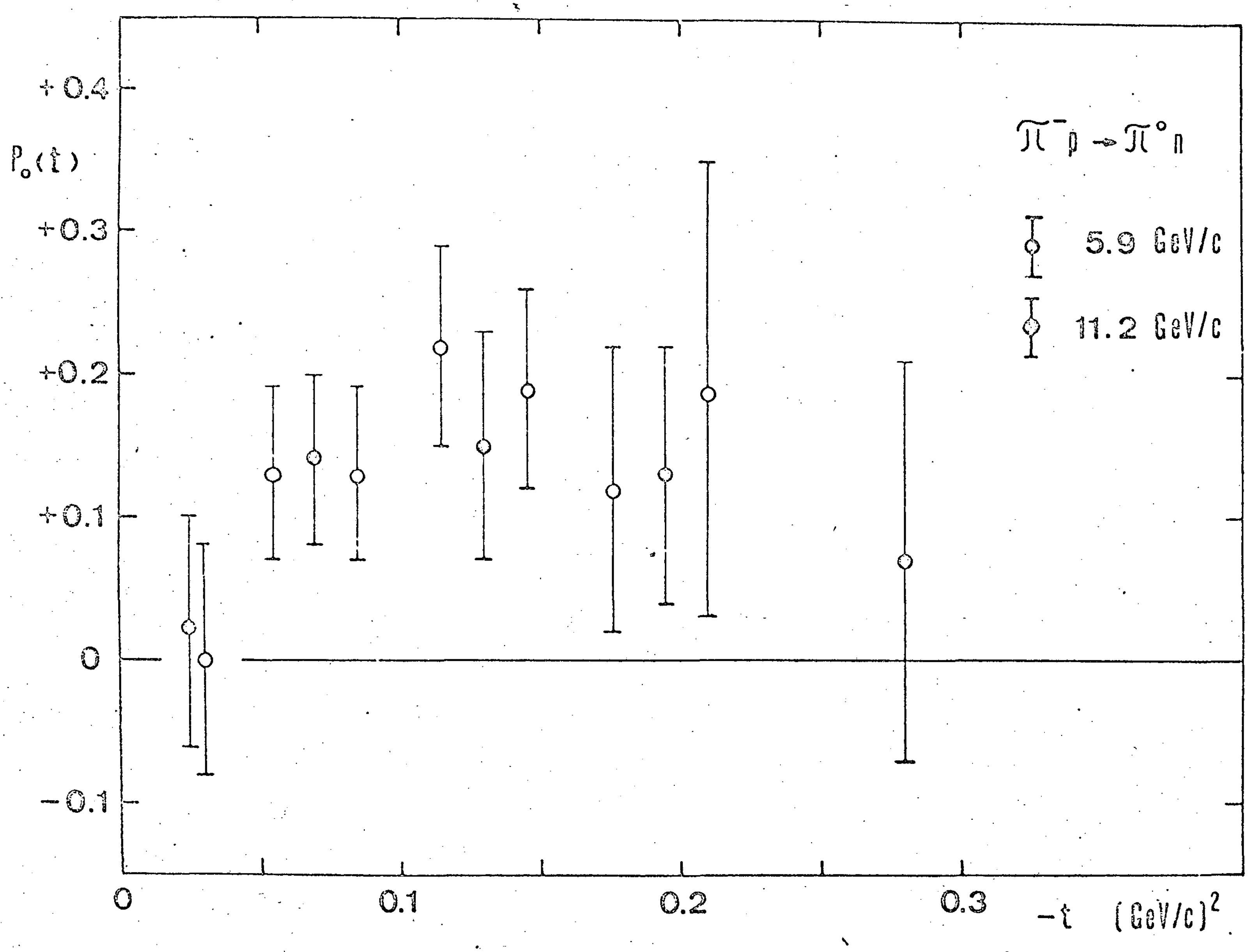

+0.4
$P_o(t)$
+0.3
+0.2
+0.1
0
−0.1
0
0.1
0.2
0.3
$-t$ $(GeV/c)^2$
$\pi^- p \to \pi^\circ n$
5.9 GeV/c
11.2 GeV/c

Fig. 27

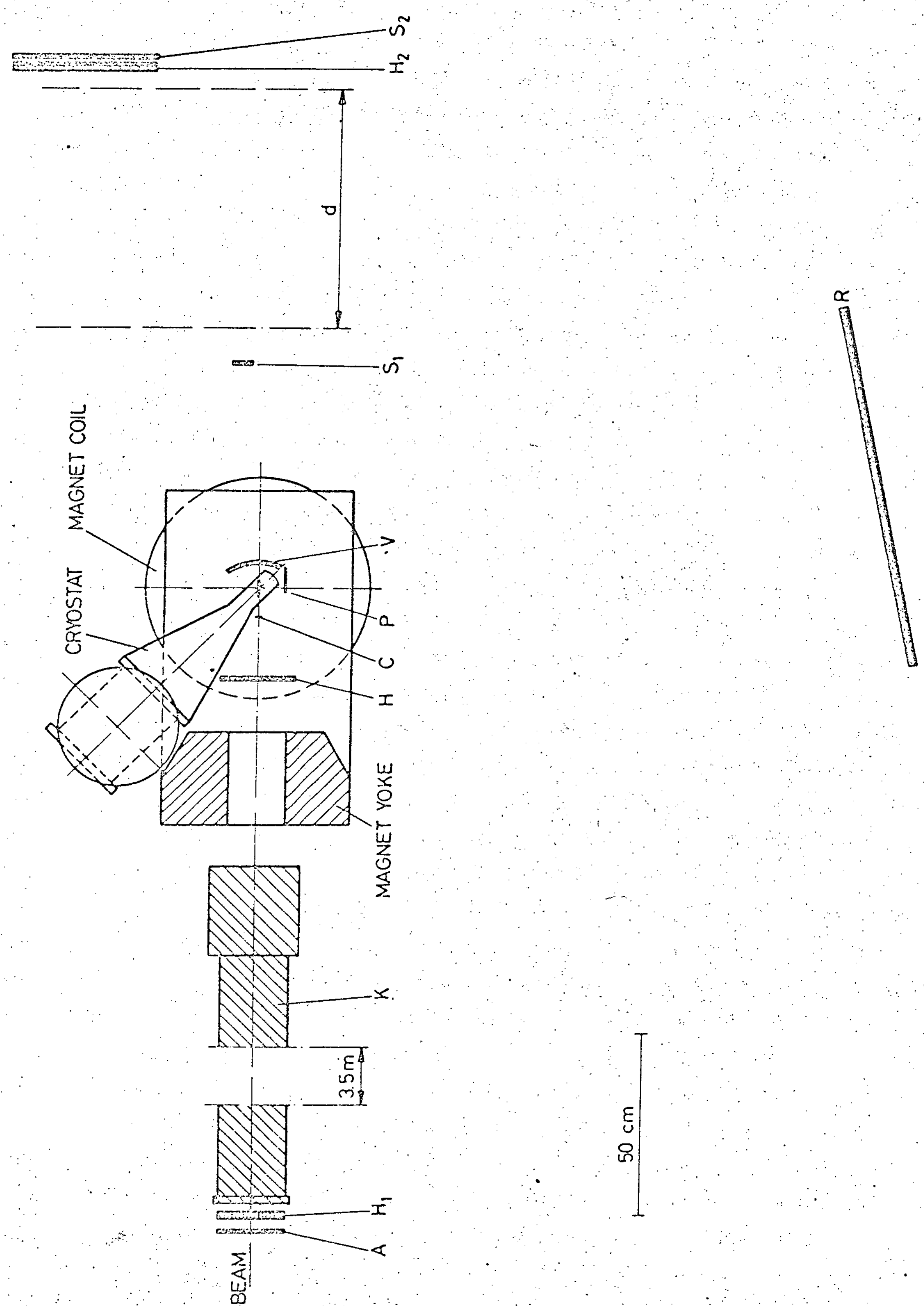
S2
H2
d
S1
MAGNET COIL
CRYOSTAT
V
P
C
H
MAGNET YOKE
K
3.5 m
H1
A
BEAM
50 cm
R

Fig. 28

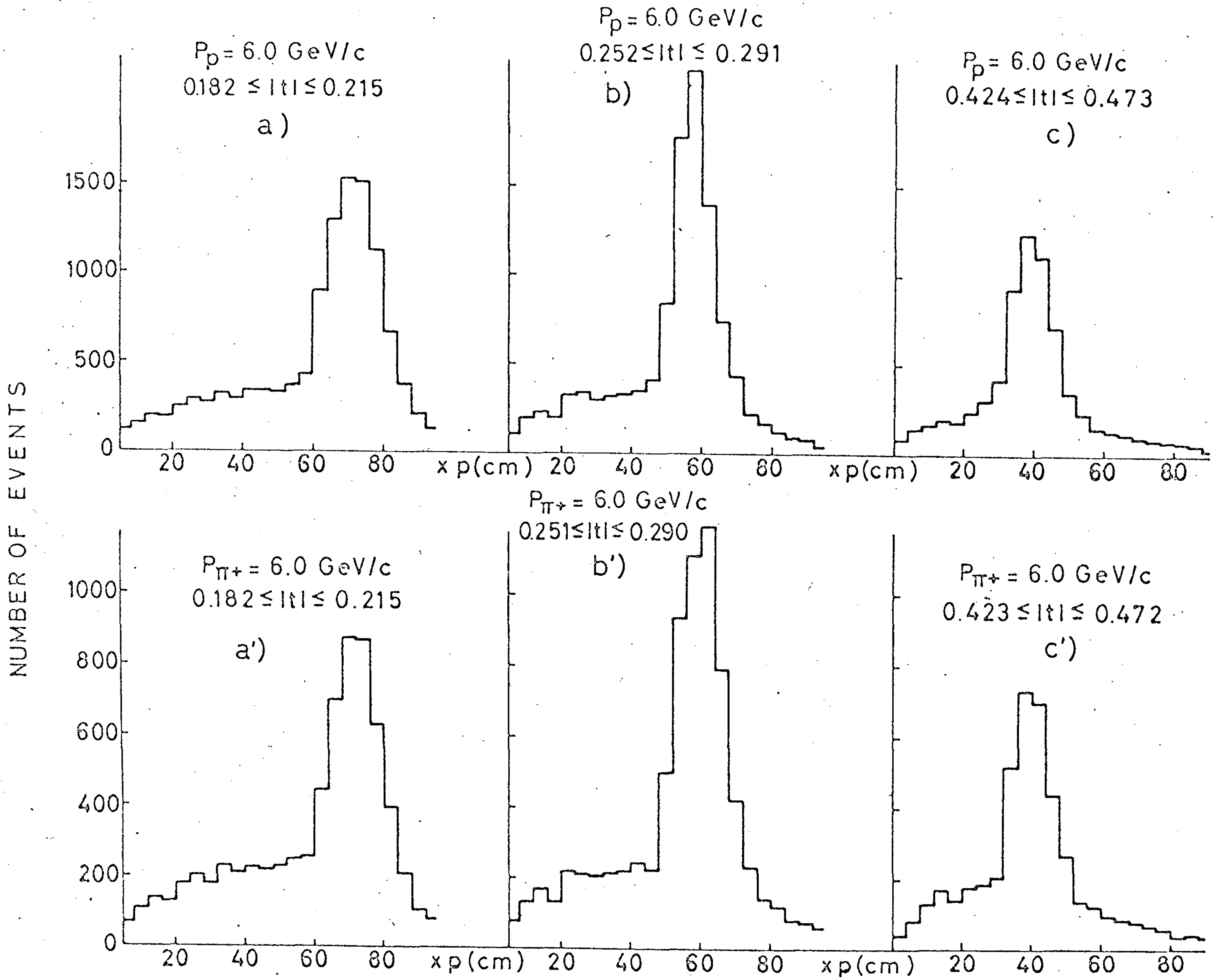
NUMBER OF EVENTS
P_p = 6.0 GeV/c
0.182 ≤ |t| ≤ 0.215
a)
P_p = 6.0 GeV/c
0.252 ≤ |t| ≤ 0.291
b)
P_p = 6.0 GeV/c
0.424 ≤ |t| ≤ 0.473
c)
$P_{\pi+}$ = 6.0 GeV/c
0.182 ≤ |t| ≤ 0.215
a')
$P_{\pi+}$ = 6.0 GeV/c
0.251 ≤ |t| ≤ 0.290
b')
$P_{\pi+}$ = 6.0 GeV/c
0.423 ≤ |t| ≤ 0.472
c')
x p(cm)
0
500
1000
1500
200
400
600
800
20
40
60
80

Fig. 29

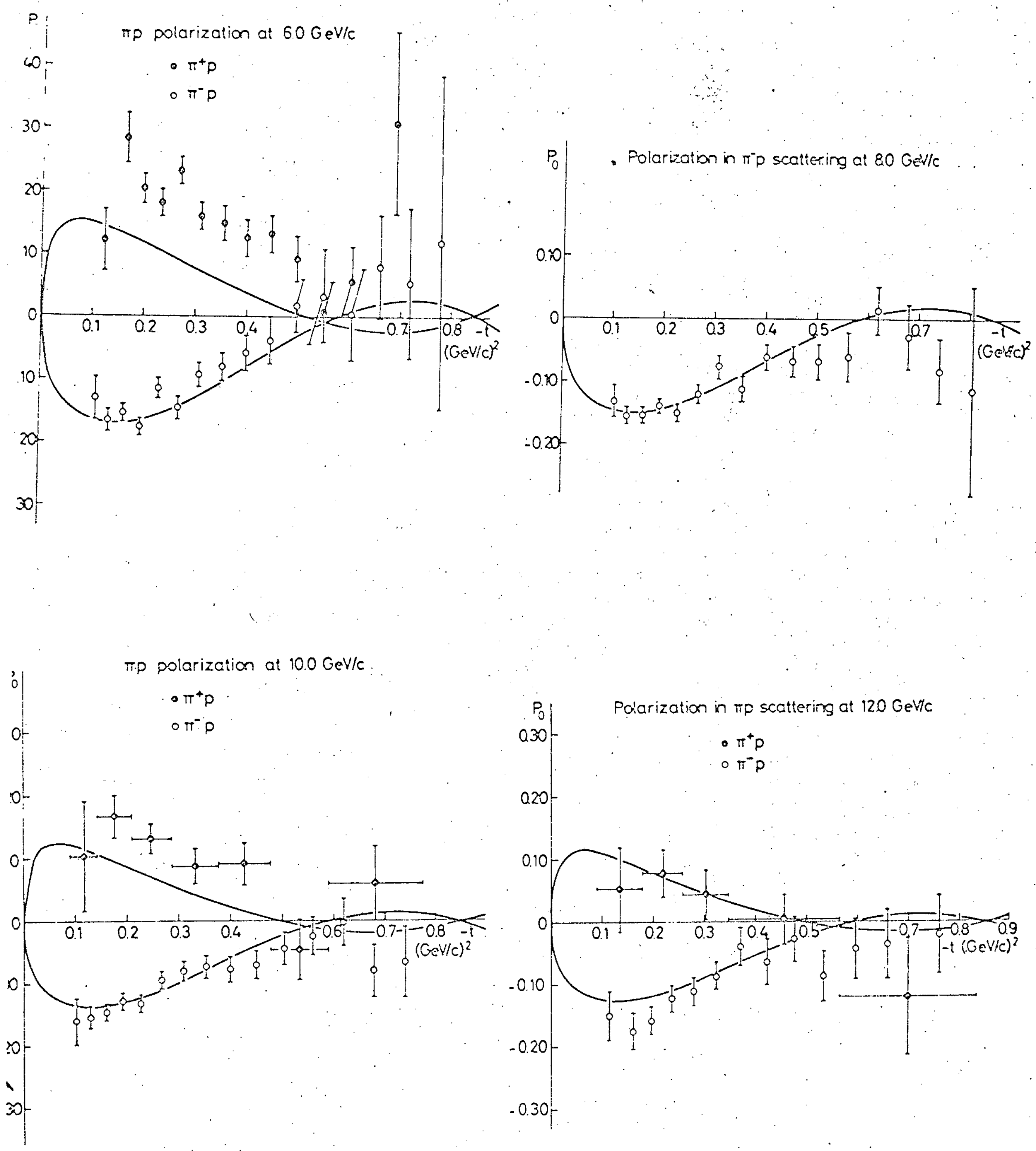
πp polarization at 6.0 GeV/c
π⁺p
π⁻p
Polarization in π⁻p scattering at 8.0 GeV/c
πp polarization at 10.0 GeV/c
π⁺p
π⁻p
Polarization in πp scattering at 12.0 GeV/c
π⁺p
π⁻p
-t (GeV/c)²

Fig. 30

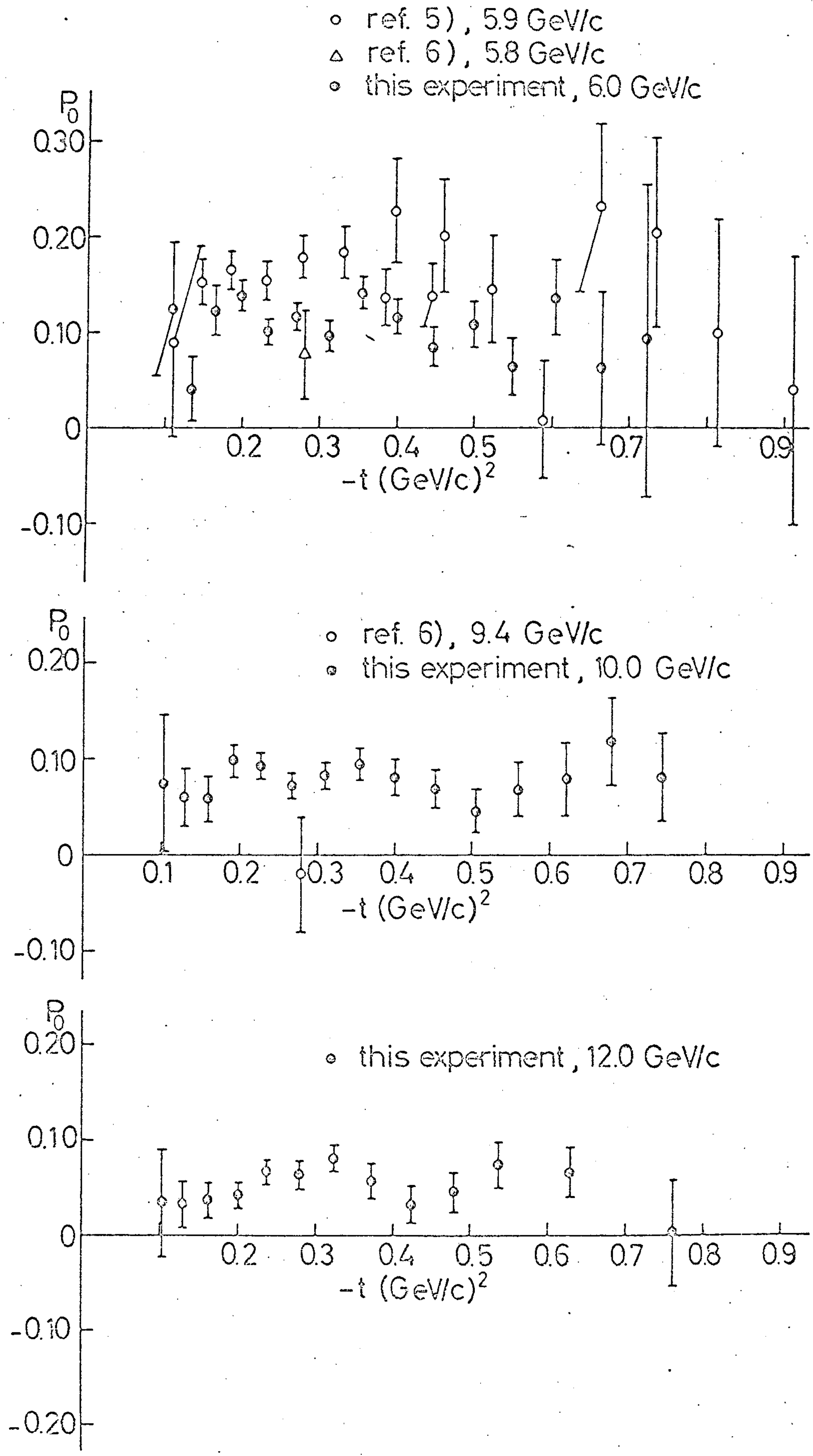
ref. 5), 5.9 GeV/c
ref. 6), 5.8 GeV/c
this experiment, 6.0 GeV/c
P_0
0.30
0.20
0.10
0
-0.10
0.2
0.3
0.4
0.5
0.7
0.9
$-t\ (GeV/c)^2$
ref. 6), 9.4 GeV/c
this experiment, 10.0 GeV/c
P_0
0.20
0.10
0
-0.10
0.1
0.2
0.3
0.4
0.5
0.6
0.7
0.8
0.9
$-t\ (GeV/c)^2$
this experiment, 12.0 GeV/c
P_0
0.20
0.10
0
-0.10
-0.20
0.2
0.3
0.4
0.5
0.6
0.7
0.8
0.9
$-t\ (GeV/c)^2$

Fig. 31